TU Delft

Delft University of Technology

Document Version
Final published version

Licence
CC BY

Citation (APA)
Nimmo, F., Ermakov, A., Kang, W., Rovira-Navarro, M., Tobie, G., & Van Hoolst, T. (2026). Internal Structure and Dynamics of the Galilean Satellites. *Space Science Reviews*, *222*(4), Article 50. https://doi.org/10.1007/s11214-026-01293-8

Important note
To cite this publication, please use the final published version (if applicable).
Please check the document version above.

Copyright
In case the licence states “Dutch Copyright Act (Article 25fa)”, this publication was made available Green Open Access via the TU Delft Institutional Repository pursuant to Dutch Copyright Act (Article 25fa, the Taverne amendment). This provision does not affect copyright ownership.
Unless copyright is transferred by contract or statute, it remains with the copyright holder.

Sharing and reuse
Other than for strictly personal use, it is not permitted to download, forward or distribute the text or part of it, without the consent of the author(s) and/or copyright holder(s), unless the work is under an open content license such as Creative Commons.

Takedown policy
Please contact us and provide details if you believe this document breaches copyrights.
We will remove access to the work immediately and investigate your claim.

This work is downloaded from Delft University of Technology.

Space Science Reviews (2026) 222:50
https://doi.org/10.1007/s11214-026-01293-8

Internal Structure and Dynamics of the Galilean Satellites

Francis Nimmo[1] · Anton Ermakov[2] · Wanying Kang[3] · Marc Rovira-Navarro[4] · Gabriel Tobie[5] · Tim Van Hoolst[6,7]

Received: 16 April 2025 / Accepted: 26 March 2026
© The Author(s) 2026

Abstract
We review the key observations and theories relevant to the internal structure and dynamics of the Galilean satellites. Key observations include: the bulk densities and degree-two gravity coefficients of the moons; the presence of conductive subsurface layers, as inferred from magnetic induction; and the surface compositions. All the moons, with the possible exception of Callisto, appear to be differentiated (denser components have separated from lighter components). Ganymede and Io have iron cores; Europa may have one. The outer three moons all likely possess subsurface oceans; for Europa the ocean overlies rock, while for the other two it overlies higher-pressure ice phases. Io is partially molten but does not possess a shallow magma ocean. Tidal heating is the dominant energy source at Europa and Io, and may have affected Ganymede's long-term evolution. The dynamics of the subsurface oceans are of considerable theoretical interest but are only weakly tied to current or likely future observations. We identify seven outstanding questions regarding internal structures, some of which will be answered by the forthcoming *JUICE, Europa Clipper* and *Tianwen-4* missions.

Keywords Satellites · Interiors · Differentiation · Tidal response · Magnetic fields

1 Introduction

Despite intensive investigation by the *Voyager* and *Galileo* spacecraft, the Galilean moons are still only partially understood. Their present-day structures and dynamics — the focus of this article — are not fully characterized, which means in turn that their origin and evolution (discussed in Nimmo et al. 2026) are shrouded in uncertainty. As summarized in Schubert et al. (2004), their bulk structure, differentiation state and the presence or absence of oceans are at least partly known, but first-order questions, such as whether Callisto is differentiated, remain. More general summaries of our knowledge of Ganymede and Europa may be found in Volwerk et al. (2025) and Pappalardo et al. (2009), respectively.

The aim of this article is threefold: to summarize our existing state of knowledge (Sects. 2 & 3); to identify key questions that forthcoming measurements by the *JUICE*, *Europa Clipper* and *Tianwen-4* missions will enable (Sects. 4-6); and to identify longer-term questions which will require future missions to answer (Sect. 7).

Extended author information available on the last page of the article

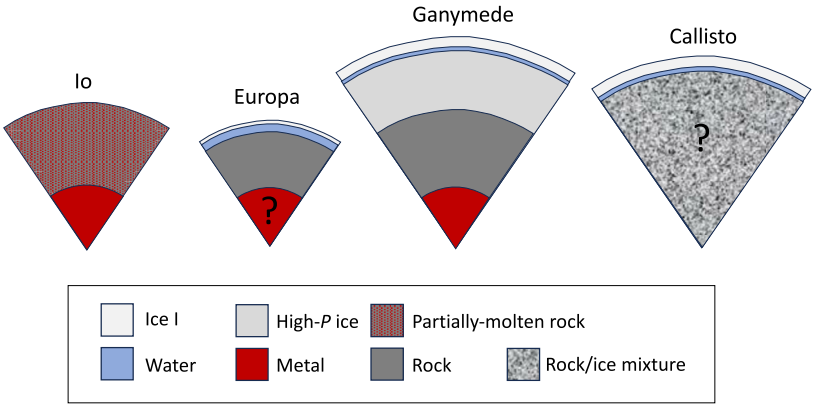

Fig. 1 Current knowledge of internal structures. Satellites and layers are at the correct relative scales. For more details see Sects. 2.3-2.6

2 Current Understanding of Internal Structures

Here we summarize our existing knowledge of internal structures, based on current observation and theory; Fig. 1 provides a graphical depiction. An excellent summary that covers much of the same ground may be found in Schubert et al. (2004). Forthcoming measurements that have not yet been performed are discussed in Sect. 4 below.

2.1 Existing Observations

The observations listed below are derived mainly from the *Galileo* mission, though some more recent data acquired by *Juno* are also relevant.

Gravity The Doppler shift of signals transmitted by the spacecraft during a flyby are used to calculate its line-of-sight acceleration. With a sufficiently good understanding of the spacecraft trajectory, the measured acceleration can be converted into an estimate of the mass and higher-order gravity moments of the body in question. The spherical harmonic degree l to which the gravity can be expanded depends on the number and geometry of the flybys. For most Galilean satellites, only the $l = 2$ gravity coefficients are currently known. These can be used to make inferences about differentiation state of the satellites and their moments of inertia (MoI) (see below). However, in order for the MoI to be determined from the $l = 2$ field and to be interpreted correctly, the satellite must be in hydrostatic equilibrium, that is, responding like a fluid. To test whether it is in hydrostatic equilibrium, both the polar (J_2) and the equatorial (C_{22}) gravity moments need to be measured. A ratio of $J_2/C_{22} = 10/3$ indicates hydrostatic equilibrium (neglecting small corrections for rapid rotation; Tricarico 2014). However, if only one moment is measured then hydrostaticity has to be assumed and so the derived MoI may not be correct (see Sect. 4.1). This situation is particularly important for Callisto.

Satellites experience time-varying tides. The gravity response of the satellite to these tides is quantified by the dimensionless tidal Love number k_2, which provides information on its density structure and rheologic profile (Sect. 4.2). So far, k_2 has only been measured for Io (Park et al. 2025a), where the tidal deformation is expected to be largest.

Table 1 Relevant satellite parameters. Square brackets indicate that hydrostatic equilibrium ($J_2 = 10/3C_{22}$) was assumed in determining J_2 and C_{22}. All MoI values are based on the assumption of hydrostatic equilibrium. The uncertainty in density is typically dominated by the uncertainty in mean radius. References: 1= Schubert et al. (2004) 2= Park et al. (2025a) 3= Nimmo et al. (2007) 4= Casajus et al. (2021) 5= Gomez Casajus et al. (2022)

Body	Bulk density kg m^{-3}	Mean radius km	J_2 (10^{-6})	C_{22} (10^{-6})	MoI	Notes
Io	3527.5±2.9	1821.6±0.5	1834.6±1.5	549.6±0.3	0.3782±0.0002	1,2
Europa	3013±1.7	1560.8±0.3	437.6±77.5	138.62±2.44	0.3547±0.0024	3,4
Ganymede	1942±4.8	2631.2±1.7	133.0±6.8	39.56±1.73	0.3161±0.004	1,5
Callisto	1834±3.4	2410.3±1.5	[32.7±0.8]	10.2±0.3	[0.3459±0.0042]	1

Shape and Topography The mean radius, long-wavelength shape and short-wavelength topography of an object can all be determined from images. The long-wavelength shape is determined from limb profiles (e.g. Thomas et al. 1998) or based on a control point network (e.g. Davies et al. 1998); short wavelength topography is based mainly on stereogrammetry or photoclinometry (e.g. Schenk et al. 2024), but suitable *Galileo* imaging coverage was very sparse. Just as they exhibit time-variable gravity in response to tides, so satellites will exhibit time-variable deformation as described by the h_2 Love number. So far, this has not been measured.

Bulk Density Given the mass and shape, the bulk density can be derived (Table 1). In the case of the Galilean satellites, the result is a monotonic decrease in density with increasing semi-major axis. This is interpreted as a monotonic increase in the ice:rock ratio, which may place constraints on how and where the different bodies formed (see Nimmo et al. 2026).

Magnetic Fields and Induction One use of magnetic field measurements is to look for a permanent field (as at Ganymede), indicative of either an active dynamo or strongly magnetized rocks.

Another use is to look for time-varying fields, that is an induction signal. Because Jupiter's magnetic dipole is tilted relative to its rotation axis, the strong magnetic field sweeps past the satellites each Jupiter rotation. The satellites thus experience a changing magnetic field. If the satellites contain a strong electrical conductor, the induced current will generate a secondary magnetic field, opposing the original field and also time-varying. This time-varying induced field can be characterized by spacecraft flybys and provides constraints on the internal conductivity structure of the moon, such as whether an ocean is present (e.g. Khurana et al. 2002).

Astrometry Measurements of the orbital migration of a moon, using spacecraft and ground-based observations, can in some circumstances be used to make inferences about its interior structure. This is because the rate at which a satellite drifts inwards and damps its eccentricity depends on the rate of tidal dissipation inside the body, which depends on its internal structure (Sect. 2.2).

Composition Spectroscopy can provide information on the surface composition of these bodies and at least some hints as to their internal make-up (e.g. Carlson et al. 2009). The moons except Io exhibit surfaces of water ice plus non-ice component(s) of uncertain origin. A complication with interpreting the surface composition is that it may have been polluted (e.g. by compounds from Io) and/or processed (e.g. by energetic particle bombardment).

As a result, detailed information on the composition of the satellite interiors is lacking. Although normally assumed to be an ice-rock-metal mixture, it is possible that carbon compounds are also present in significant quantities (Reynard and Sotin 2023), in which case the conventional pictures of internal structure will be incorrect. Even in the absence of carbon, the silicates might include clays (Mousis et al. 2023), which would make inference of rock:ice ratios more complicated.

Microwave Radiometry Microwave radiometry is a passive technique whereby the spectral radiance of a body (expressed as a brightness temperature) is measured. Since different frequencies probe to different target depths, a physical temperature gradient will give rise to different brightness temperatures at different frequencies. Thus in principle the temperature gradient (and hence the heat flux) can be measured. However, the penetration depth is sensitive to impurities (such as salts), and the spectral radiance will also depend on the degree of scattering in the target. At the Jupiter system, external sources of radiation (e.g. synchrotron radiation) also have to be accounted for in analyzing the measurements. The *Juno* microwave radiometer (MWR) has imaged Ganymede, Europa and Io. So far, the biggest challenge in interpreting these results has been the effect of contaminants and scattering. To some extent these can be corrected for by measuring the emission angle dependence of the brightness temperature (i.e., limb darkening), but the resulting uncertainties in the inferred heat flux are large (Brown et al. 2023).

2.2 Theoretical Constraints on Internal Structure

A central question concerning the Galilean satellites is the extent to which they have undergone differentiation. The reason this is important is because it constrains how they formed (Nimmo et al. 2026). Here, differentiation means both separation of ice from rock, and also separation of rock from metal. The latter is more difficult to achieve than the former because differentiation requires at least partial melting, and metal requires higher temperatures to melt than ice. The internal temperature structures of these bodies are hard to determine via observation, with the possible exception of MWR or future sounding radar measurements (Sect. 4.5). As a result, theory is used.

As discussed in Nimmo et al. (2026) there are three possible sources of energy capable of causing differentiation: accretion heating, radiogenic heating, and tidal heating. Except in unusual circumstances, accretion heating should be sufficient to cause ice-rock differentiation, but not rock-metal differentiation. Radiogenic heating is marginally capable of causing the latter but depends on whether heat is being transported by conduction or advection.

Tidal heating is more complicated because it both depends on, and affects, the internal structure of the body. The rate of tidal heating $\dot{E}$ is given by (Wisdom 2008)

$$\dot{E} = \frac{3}{2}\frac{n^5 R^5}{G}\frac{k_2}{Q}\left(7e^2 + \theta^2\right) \tag{1}$$

where n is the mean motion, R the radius, e the eccentricity and θ the obliquity of the moon, G the gravitational constant and this expression is valid for small e and θ. The quantity k_2/Q describes the amplitude and phase lag of the tidal response, and depends on the internal structure of the body (e.g., whether an ocean is present), the forcing frequency and rheological properties (e.g. rock is more rigid than ice).

Tidal heating also damps the body's eccentricity. The reason that the eccentricities of Io and Europa are non-zero is because they are being excited by the 1:2:4 Laplace resonance

among the inner three satellites.[1] This resonance is the ultimate cause of the vigorous activity on Io and (to a lesser extent) Europa.

The internal structure of a body controls not only the magnitude of tidal heating (equation (1)) but also its spatial distribution (e.g. Ross et al. 1990). For instance, tidal heating in an ice shell results in higher heat fluxes at the poles. Thus, if direct or indirect inferences of the heat flux distribution can be acquired, that constrains the internal structure.

Transport of the heat generated by one of these three mechanisms can be either by conduction or advection. Conduction is straightforward to model; a minor complication is that ice becomes progressively more thermally conductive at lower temperatures (Petrenko and Whitworth 1999). One form of advection is convection, whereby thermal buoyancy contrasts produce motion which advects the heat vertically. Whether convection occurs depends on the Rayleigh number Ra, given by

$$Ra = \frac{\rho g \alpha \Delta T d^3}{\kappa \eta} \tag{2}$$

Here ρ, α, κ and d are the density, thermal expansivity, thermal diffusivity and thickness of the convecting medium. The temperature contrast across the layer is ΔT, the gravity is g and η is the viscosity (at the base of the layer if the viscosity is temperature-dependent; Solomatov 1995). Both rock and ice have strongly temperature-dependent viscosities, so the minimum Ra needed to permit convection is of order 10^8 and 10^5, respectively (e.g. McKinnon 2006).

On Earth, rock near its melting point has viscosities of order 10^{20} Pa s; the resulting value for Ra suggests that the mantles of the Galilean satellites are unlikely to be convecting. Ice-I has a much lower viscosity, of order 10^{14} Pa s (Goldsby and Kohlstedt 2001). An ice shell of thickness 30 km is therefore quite likely to be convecting, while one of 10 km thickness is not. Higher pressure ice phases tend to have higher viscosities (Durham et al. 2010).

Because Ice-I has a low viscosity, lateral shell thickness contrasts tend to be rapidly smoothed out by flow in the lowermost part of the ice shell (Nimmo 2004a). This process does not advect much heat, but it is an important process to consider when looking at how shell thickness contrasts evolve in response to variable bottom heating (Sect. 3.2).

In addition to convection, heat can also be advected via melt transport. Water, being denser than ice, is hard to erupt unless external stresses (Manga and Wang 2007) or volatile exsolution (Crawford and Stevenson 1988) are invoked. Magma, however, is less dense than rock, so that heat transfer via melt ascent is a potentially important mechanism in the silicate portions of heated moons. The rate of separation of melt from solid is a strong function of the melt viscosity and melt fraction (e.g. Miyazaki and Stevenson 2022); at some depth, melt transport by permeable flow is superseded by melt transport in macroscopic fractures i.e. dikes.

An important set of theoretical constraints arises from the peculiar phase diagram of ice (e.g. Journaux et al. 2020). Ice at low pressures (Ice-I) has a melting temperature that decreases with increasing pressure; as a consequence, water is denser than Ice-I. This behaviour has important consequences for possible ocean dynamics (Sect. 3.2). At higher pressures, ice forms phases that are denser than water. Consequently, large icy moons can produce an "ice sandwich": a deep layer of high-pressure ice, an intermediate layer of liquid water, and then a top layer of Ice-I.

[1] Ganymede is part of the Laplace resonance but its eccentricity is not being excited significantly.

2.3 Io

Io's density implies a rock-iron mixture. Both $l = 2$ gravity moments are known, and confirm that Io is in hydrostatic equilibrium. As a result, its MoI is known, demonstrating that Io is differentiated and allowing constraints on its core radius (650-950 km) and density to be obtained (Schubert et al. 2004). Induction measurements suggest that Io is highly conductive; because rock conductivity increases significantly on melting, this observation has been interpreted as requiring a silicate melt fraction of at least 20% (Khurana et al. 2011). Surprisingly, however, Io does not appear to possess a subsurface magma ocean. Recent measurements of its tidal response k_2 reveal a value of 0.125 ± 0.047, too small for a shallow magma ocean (Park et al. 2025a) but consistent with predictions assuming a partially-molten mantle (Bierson and Nimmo 2016). Astrometry (Lainey et al. 2009) and gravity (Park et al. 2025a) have both been used to measure k_2/Q and yield a value of about 0.015. This value, when inserted into equation (1), produces a power output comparable to that measured via infra-red measurements (Veeder et al. 1994). This agreement suggests that Io is currently in steady-state: it is producing as much heat as it is releasing. The mechanism by which Io transports this heat to the surface is dominated by advection - Io is a "heat-pipe" planet, as first recognized by O'Reilly and Davies (1981). It is presumably the rapid transport of melt from the interior to the near-surface that frustrates the development of a fully-molten magma ocean (Miyazaki and Stevenson 2022). A consequence of this heat-pipe process is that the crust of Io is cold and capable of maintaining significant topography (as observed; Schenk and Bulmer 1998).

2.4 Europa

Europa's high bulk density implies that the observed surface hydrosphere cannot be very thick. Although the equatorial gravity moment C_{22} is well-constrained, the polar moment (J_2) is not. Thus, we cannot be sure that Europa is in hydrostatic equilibrium. Assuming it is, the inferred MoI is 0.3547 ± 0.0024 (Casajus et al. 2021).[2] The implied H_2O thickness is then roughly 140 km. Europa's strong magnetic induction signature indicates that part of the H_2O is both liquid and at least slightly salty (Zimmer et al. 2000). The presence of NaCl at the surface is likely the result of eruptions from this subsurface ocean (Trumbo et al. 2019). The thickness of the ice shell is quite uncertain, although impact simulations suggest that it is in excess of 20 km (Turtle and Pierazzo 2001; Wakita et al. 2024). Whether Europa has a metallic core is uncertain; the most recent MoI value suggests that the core might be quite small (Petricca et al. 2025a) but such determinations are non-unique (Schubert et al. 2009). Another uncertainty concerns the mantle. Radiogenic heating is not guaranteed to cause rock-metal differentiation (Trinh et al. 2023) but the degree of tidal heating in the mantle - and thus the mantle temperature - is unknown.

2.5 Ganymede

Ganymede's bulk density implies a roughly 50% ice mass fraction, indicating that both ice I and higher-pressure phases will be present. It possesses a permanent dipole moment (Kivelson et al. 2002), interpreted as the field generated in a convecting metallic core. Since Ganymede's surface is icy, it appears to have undergone complete ice-rock-metal differentiation. The gravity moments are compatible with hydrostatic equilibrium and the inferred

[2]Note that this estimate is larger by several σ from earlier estimates.

MoI is consistent with a fully-differentiated object (Gomez Casajus et al. 2022). There also appear to be regional gravity anomalies, perhaps reflecting mass anomalies in the mantle or ice (Palguta et al. 2006). In addition to the permanent dipole, Ganymede also displays an induction component indicating the presence of a sub-surface ocean (Kivelson et al. 2002). This ocean presumably resides between the ice I shell and the deeper, high-pressure ice phases below. *Juno* MWR observations suggest that the maximum conductive shell thickness is 150 km (Brown et al. 2023); but this conclusion is for a pure ice shell, which may not be a good assumption Phua and Stevenson (2026). Surface observations suggest that Ganymede underwent a strong reheating event mid-way through its evolution (Pappalardo et al. 2004). The energy source was presumably tides, although the exact mechanism remains uncertain (Showman et al. 1997). Whether Ganymede was fully differentiated before this supposed heating event is unknown.

2.6 Callisto

With respect to differentiation, Callisto is the most puzzling of the major Galilean moons. Its similar bulk density to Ganymede implies a roughly 50% ice mass fraction. However, if it is hydrostatic, the inferred MoI implies incomplete differentiation (Schubert et al. 2004). Unfortunately, because J_2 could not be measured independently of C_{22}, whether the hydrostatic assumption is correct is not known. Thus, Callisto's differentiation state is uncertain (Gao and Stevenson 2013). A further puzzle is that Callisto exhibits a strong induction signature (Zimmer et al. 2000). Although this signature might be due to Callisto's unusually large ionosphere (Hartkorn and Saur 2017), most likely it indicates the presence of a subsurface ocean (Cochrane et al. 2025) as for Ganymede. Models that allow *both* an interior cold enough to not differentiate *and* maintenance of a shallow ocean do exist (Nagel et al. 2004) but are not very intuitive. As for Ganymede, the ice I shell thickness is likely 100-200 km and it is probably, though not certainly, convecting (McKinnon 2006). In contrast to Ganymede, Callisto shows almost no tectonic features (Greeley et al. 2000); it has apparently been largely quiescent ever since it formed, suggesting it may never have occupied a resonance with the inner satellites.

3 Current Understanding of Dynamics

Here we discuss the likely motion of the solid and fluid parts of the interiors. For the solid part, a useful general discussion may be found in Collins et al. (2009). For the fluid part, a good review is by Soderlund et al. (2024).

3.1 Solid Body Dynamics

Motion in the solid parts of the Galilean satellites are driven by stresses, which can arise from tides, buoyancy, shape changes and impacts, among other causes. We discuss each in turn.

The eccentricities of the satellites result in a time-variable tidal bulge, which in turn produces stresses. The amplitude of the diurnal tidal bulge H is (Murray and Dermott 1999)

$$H = 3eRh_2 \frac{M}{m} \left(\frac{R}{a} \right)^3, \tag{3}$$

where M and m are the mass of Jupiter and the satellite, R is the satellite radius, a its semi-major axis, e its eccentricity. The quantity h_2 is the tidal Love number describing deformation. The resulting diurnal elastic stress σ is then given by Wahr et al. (2009)

$$\sigma \approx 3eh_2\mu \frac{M}{m}\left(\frac{R}{a}\right)^3 = 3eh_2\mu \frac{n^2 R}{g}, \tag{4}$$

where g is the surface gravity, n the mean motion and μ the rigidity of the deforming layer. For Europa, with $e \approx 0.01$, $h_2 \approx 1.2$ (Moore and Schubert 2000) and $\mu = 3$ GPa (for ice), the diurnal stresses are roughly 60 kPa. Stresses are about the same at Io, because of its smaller eccentricity and Love number (h_2 is not measured but based on the measured k_2 is expected to be roughly 0.2). The low eccentricity of Ganymede and the large semi-major axis of Callisto result in stresses smaller by more than an order of magnitude for these two bodies (Collins et al. 2009).

Tidal stresses may drive deformation. In particular, their cyclic nature may drive so-called "tidal walking" (Hoppa et al. 1999a), potentially responsible for the strike-slip faults seen on Europa; diurnal tides might also have caused the peculiar cycloids observed there (Hoppa et al. 1999b). Tidal stresses also, indirectly, generate heat (Eq. (1)). This heat causes volcanism on Io, could drive convection in Europa's ice shell (Sect. 2.2), and is likely responsible for the resurfacing inferred on Ganymede.

Convection (Sect. 2.2) is driven by thermal buoyancy. While tidal heating is one source of energy, another is radioactive decay, which could drive convection in the ice shells of Ganymede and Callisto. Although the silicate mantles of these bodies are probably too viscous to convect, thermally-driven circulation of water infiltrated into the shallow, permeable parts of these mantles may occur (Vance et al. 2007). Compositional buoyancy is responsible for the eruption of melts on Io, while "cryovolcanism" elsewhere is impeded by the higher density of water relative to ice I.

Global changes in shape can give rise to large stresses. Non-synchronous rotation, driven by either tides or ocean currents (Sect. 3.2) involves motion of the solid surface relative to the tidal bulge. Stresses depend on the amount of rotation but can easily reach many MPa (Collins et al. 2009). Polar wander can be driven by shell thickness variations (Ojakangas and Stevenson 1989); it also involves relative motion of the surface and bulge, and can generate MPa-level stresses. There is some evidence that this has actually happened on Europa (Schenk et al. 2020). Finally, as an ice-I shell thickens, the surface must move outwards (because ice takes up more volume than water), resulting in global expansion, large (MPa-level) stresses (Nimmo 2004b) and ocean pressurization, potentially causing cryovolcanism (Manga and Wang 2007). These volume-change effects are much less pronounced for Ganymede and Callisto because the higher pressure ice phases counteract the effect of ice-I.

Finally, bolide impacts impart local, initial stresses up to the TPa level. The long-term crater left by an impact results in long-term, MPa-level stresses which can lead to flow in the ice shell and viscoelastic relaxation of the crater over geological time (e.g. Dombard and McKinnon 2006).

3.2 Ocean Dynamics

Icy moons' subsurface oceans are inherently difficult to probe directly. To make progress, we have to build connections between ocean properties and ocean circulation with potential observables. As a fluid layer, the subsurface ocean can actively redistribute heat across different latitudes and longitudes and transport momentum between the ice shell and silicate

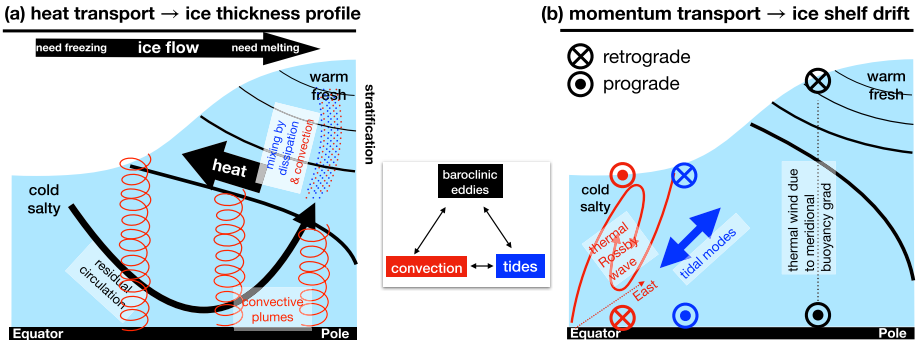

Fig. 2 Schematics for ocean dynamics and the induced (a) heat transport and (b) momentum transport. Processes associated with convection, baroclinic eddies and tides are denoted by red, black and blue colors, respectively. Detailed discussion can be found in the text

core. The former influences the ice thickness profile (e.g., Soderlund et al. 2014; Kvorka et al. 2018; Kang and Jansen 2022; Kang 2022; Kang et al. 2022; Lemasquerier et al. 2022; Kvorka and Čadek 2024; Gastine and Favier 2024), while the latter affects the librational and non-synchronous rotation (NSR) motions of the ice shell (Ashkenazy et al. 2023; Hay et al. 2023; Kang 2024; Hay et al. 2024). Both are potentially measurable by upcoming missions though not available at present. These observations can potentially be converted to constraints on ocean heat and momentum transport, and thereby constraints on the ocean properties and dynamics. In principle, fluid flows in the ocean will give rise to additional magnetic induction signals (Tyler 2011b), but these are likely too small to measure (Šachl et al. 2025), except perhaps for Ganymede where a strong intrinsic field is present.

Subsurface oceans on icy satellites are usually subject to three types of forcing as sketched in Fig. 2. The first type of forcing is heating from the bottom silicate core (Choblet et al. 2017). When thermal expansivity is positive,[3] the heating drives *convective motions* (red notations in Fig. 2) that transmit heat from the silicate core to the ice shell while inducing efficient vertical mixing (Soderlund et al. 2014, 2020; Bire et al. 2022; Lemasquerier et al. 2022; Zeng and Jansen 2024). The rotationally constrained convective dynamics in polar regions differ from those in equatorial regions: in polar areas, convection manifests as spiral plumes along the rotational axis (red spirals in Fig. 2a), while in equatorial regions, it appears as overturning rolls along the equatorial plane (red arrows in Fig. 2b). Depending on which form of convection is more efficient in heat transport, up to ∼20% heat may be redistributed across different latitudes (Amit et al. 2020; Kvorka and Čadek 2022; Gastine and Aurnou 2023; Bire et al. 2022). The equatorial rolls, known as thermal Rossby waves, can transport eastward momentum toward the surface and drive nonsynchronized rotation of the ice shell (see Fig. 2b, Ashkenazy et al. 2023; Hay et al. 2023).

The second type of forcing is the heat and salinity fluxes from the ice shell. When ice thickness is non-uniform, the temperature at the water-ice interface will vary with the local pressure (lower beneath thicker ice), following the Clausius-Clapeyron relationship. In addition, freezing in thick ice regions and melting in thin ice regions are required to maintain the ice thickness variations against lateral ice flow (Sect. 2.2), making water under thick ice saltier than elsewhere (see Fig. 2a, Lobo et al. 2021; Zhu et al. 2017; Kang et al. 2022;

[3]This generally holds for Galilean moons as high pressure suppresses water's anomalous expansion near freezing point.

Ashkenazy and Tziperman 2021). These horizontal temperature and salinity gradients excite *baroclinic eddies*. The transport effect of these eddies can be equivalently represented by an overturning circulation that sends dense water downward (black arrow in Fig. 2a). They mix the cold water under thick ice with the warm water under thin ice, leading to heat transport toward thick ice regions and reducing the ice thickness variations (Zhang et al. 2024; Kang 2022). Also, they may fill the bottom ocean with dense fluid, harvesting energy and creating stratification near the surface (black curves in Fig. 2 show density contours, Kang 2023). In fact, Earth's ocean and atmosphere are both strongly stratified as a result of the baroclinic adjustment triggered by the poleward cooling trend.

The third type of forcing is mechanical forcing arising from tides and changes in the spin of the moons (i.e., libration, precession), which drive ocean currents that induce momentum transport and ocean dissipation (Soderlund et al. 2024). As for terrestrial oceans, we can distinguish between barotropic (no vertical structure) and baroclinic (with vertical structure) ocean currents. Barotropic tides are characterized by surface and Rossby waves. As the former propagate much faster than the diurnal tidal potential, the ocean quickly adapts to the perturbation and nearly follows the time-changing geoid (e.g., Beuthe 2016). As a consequence, the amplitude of these waves is small, unless the ocean is very thin. This is not the case for the higher frequency of moon-moon tides, which can resonantly excite surface gravity modes (Hay et al. 2020). Rossby waves can be efficiently excited and drive strong ocean currents (e.g., 0.1 m/s for Europa) in cases when the obliquity of the moons is high (Sect. 4.3.2) and the ocean of constant thickness (Tyler 2008; Chen et al. 2014; Rovira-Navarro et al. 2020).

Beyond barotropic waves, the oceans' stratification in angular momentum means that they also support internal inertial waves. These waves can form internal shear layers that focus energy dissipation (Rovira-Navarro et al. 2019; Rekier et al. 2019). If oceans are also stratified in density, internal gravity waves are also expected. Such waves propagate slower than surface gravity waves and can be resonantly excited by the diurnal tide, causing significant tidal dissipation and surface deformation (Tyler 2011a; Rovira-Navarro et al. 2023; Idini and Nimmo 2024). The flow of the barotropic tide over topography can also produce internal waves, a process that accounts for $\sim 30\%$ of the energy dissipated in the Earth's ocean (Garrett and Kunze 2007). Similar processes might occur at the seafloor and ice-bottom interfaces of the Galilean satellites, though the topography and roughness of these surfaces is unknown. Variations of the waves mentioned above are prone to instabilities that can lead to ocean mixing. Internal gravity waves can break due to the Kelvin-Helmholtz instability; the centrifugal instability can cause shear layers forming at the ocean ice interface due to libration to break (Noir et al. 2009), potentially causing significant tidal heating (Wilson and Kerswell 2018); and the non-linear interaction of internal waves excited by tides and libration with the mean flow via the elliptical instability can cause ocean-wide turbulence (Le Bars et al. 2015; Kerswell 2002; Cebron et al. 2012; Lemasquerier et al. 2017).

While most studies have focused on dynamics due to a specific type of forcing, it is important to remember that all three types of dynamics coexist and strongly interact with one another. As one example, the stably stratified layer due to baroclinic eddies can not only shut off convective transport (height of convective plumes limited by stratification in Fig. 2a, Kang 2023) but also significantly alter the tidal response by supporting internal modes (Rovira-Navarro et al. 2023; Idini and Nimmo 2024). As another example, the vertical mixing induced by the dissipation of tidal-driven internal waves (Wunsch and Ferrari 2004) and convection (Soderlund et al. 2014) provides energy for the baroclinic residual circulation by mixing dense fluid from the bottom ocean back upward (blue/red dotted lines in Fig. 2a, Jansen et al. 2023), thereby reducing stratification. Finally, periodic tidal forcing

of the ocean can give rise to mean circulation (Hay et al. 2024), thus coupling short-period and long-period effects.

Ocean dynamics control the pattern of heat delivered to the ice shell and thereby the ice thickness profile. For instance, if part of the ice shell has a stratified ocean layer beneath it, heat will have difficulty reaching that area, as stratification can suppress convective motions and deflect heat away. Whether a stratified layer forms depends on the relative strength of baroclinic forcing, which restores stratification, and convective forcing, which destroys stratification. Following the scaling given by Kang (2023), an equator-to-pole ice thickness variation of merely 100 m on Europa can deflect around 100 mW m^{-2} of heat from reaching the thin ice regions, and consequently, the thicker ice regions receive more heat from the ocean and melt. Because even modest shell thickness variations can effectively suppress convection driven by bottom heating, the long-wavelength topography of Europa is expected to be very muted ($\sim$10 m amplitude). In contrast, spatially varying tidal dissipation generated in the ice shell can sustain ice thickness variations more effectively, as it is directly deposited into the ice (Nimmo et al. 2007).

If significant variations in ice thickness are detected, it would point to heat production being concentrated within the ice shell rather than the silicate core. It could also imply weak ocean circulation, possibly caused by low ocean dissipation or lack of heating from the silicate core or having an ocean of specific salinity levels that reduce circulation strength (Kang 2022; Zhang et al. 2024; Kang et al. 2022); the logic here is that any long-wavelength ocean circulation is expected to advect heat towards regions of thicker ice. Detection of weak ice thickness variations is less informative, as it can be explained by either dominant heat generation in the silicate core, a strong ocean circulation, and/or rapid lateral flow of the ice shell.

Ocean momentum transport can be affected by the three types of dynamics as well. As sketched in Fig. 2b, the equatorial thermal Rossby waves triggered by bottom heating have a structure that tilts eastward from the bottom to the top, which transports prograde momentum toward the surface (Busse 1970) and causes the ice shell to rotate faster than the rest of the body (Ashkenazy et al. 2023). It has also been shown in numerical simulations that a retrograde jet can form near the equator surface, but that only happens in the slow-rotating regime (Aurnou et al. 2007), which is less relevant for icy moon oceans (Bire et al. 2022; Soderlund 2019; Jansen et al. 2023). In contrast, a poleward decreasing trend of density in the ocean would require a retrograde shear to balance, according to the thermal wind equation - which should generally apply to these fast-rotating icy moon oceans (Bire et al. 2022; Soderlund 2019). This shear would cause the ice shell to rotate at a slower rate than the interior. Finally, Hay et al. (2024) showed that obliquity tidal motions do not average to zero and can also pump retrograde momentum to the surface (Fig. 2b).

Because all three types of dynamics can redistribute momentum, interpreting ocean dynamics from non-synchronous rotation (NSR) observations will involve some degeneracy, even after the direct torques on the shell from Jupiter (Greenberg and Weidenschilling 1984) and the resistance of the elastic shell to being rotated (Goldreich and Mitchell 2010) have been taken into account. Although prograde drift could be due to either Jupiter torques or convection-dominated dynamics, retrograde motion is not possible with Jupiter torques and would thus be a strong indication of ocean flow (driven by either tides or baroclinic eddies). Furthermore, a fast NSR rate induced by ocean flow would indicate strong friction near the water-ice interface, strong dissipation, and thereby a strong energy source.

The energetics of ocean dynamics provide a unique perspective for the prediction and retrieval of ocean dynamics. Following the analysis in Jansen et al. (2023), while bottom heating and mixing due to tidal dissipation both work to energize the ocean dynamics, the

heat and salinity fluxes associated with ice thickness variations do not provide much energy to drive circulation, because the buoyancy source under thin ice is located at higher elevation than the buoyancy sink under thick ice.[4] Therefore, the existence and strength of baroclinic eddies largely hinges on the extent to which the ocean's potential energy can be replenished by convection and/or by mixing due to tidal wave breaking. The percentage of heat (Q) converted into useful mechanical work (W) to sustain ocean dynamics can be as high as 20% for tides (Wunsch and Ferrari 2004), but is generally low for convection limited by the second law of thermodynamics: work (Carnot) efficiency $\eta \equiv W/Q < \Delta T/T$, where ΔT is the temperature contrast (O(1-10) mK (Gastine et al. 2016)) and T is the background temperature $\sim$ 273 K. In contrast, the high work efficiency associated with tidal motions indicates that even when its dissipative heat production is negligible, its mechanical work can sustain substantial ocean dynamics in the form of baroclinic eddies and tidal waves.

A further advantage of energetic arguments is that they can be used to place upper limits on flow speeds, irrespective of the specific flow geometries. For example, at Europa, if we assume that bottom heating is the only form of forcing, the energy input rate should be able to sustain ocean currents on the order of $O(1)$ cm/s according to Jansen et al. (2023).

4 Future Measurements

4.1 Static Gravity and Topography

A planetary shape can be represented in terms of spherical harmonic expansion:

$$r(\lambda, \phi) = R_{mean} \sum_{l=0}^{\infty} \sum_{m=0}^{l} \left[\bar{A}_{lm} \cos(m\lambda) + \bar{B}_{lm} \sin(m\lambda) \right] \bar{P}_{lm}(\sin(\phi)), \tag{5}$$

where r is the radius, ϕ is the latitude, λ is the longitude, R_{mean} is the mean radius of the body, $\bar{A}_{lm}$ and $\bar{B}_{lm}$ are the normalized spherical harmonic coefficients and $\bar{P}_{lm}$ are the normalized associated Legendre functions. The quantities l and m are the spherical harmonic degree and order, respectively. The gravitational potential can also be represented in spherical harmonics:

$$U(r, \lambda, \phi) = \frac{GM}{r} \sum_{l=2}^{\infty} \sum_{m=0}^{l} \left(\frac{R_0}{r} \right)^l \left[\bar{C}_{lm} \cos(m\lambda) + \bar{S}_{lm} \sin(m\lambda) \right] \bar{P}_{lm}(\sin(\phi)), \tag{6}$$

where R_0 is the reference radius of the gravity field model and $\bar{C}_{lm}$, $\bar{S}_{lm}$ are the normalized gravity coefficients. The shapes of tidally-locked moons are dictated by their tidal and rotational parameters, internal density distribution, and any deviations from hydrostatic equilibrium (that is, a situation in which the body is responding like a fluid). For a tidally-locked moon, tidal and rotational potentials produce a permanent bulge, which has the largest contribution for the $l = 2$ shape and gravity terms. The amount of tidal and rotational distortion is related to the internal structure and, most importantly, to the differentiation state of the moon that determines its radial density profile (Schubert et al. 2004). Both hydrostatic gravity and shape data can be used to assess the state of internal differentiation. However, as no planetary body is perfectly hydrostatic, the non-hydrostatic contributions to gravity and

[4] This would not be true if the ocean's thermal expansivity were negative - unlikely for Galilean moons.

Table 2 Summary of ellipsoidal shape parameters of the Galilean moons. *For Ganymede and Callisto the values are theoretical, based on gravity measurements, not observed. CPN=control point network. LP=limb profiles. HE=hydrostatic equilibrium assumed

Body	$a-b$ (km)	$a-c$ (km)	Comment	Reference
Io	10.7±0.5	14.5±0.5	Measured (CPN)	Oberst and Schuster (2004)
Europa	2.3±0.7	3.1±1.0	Measured (LP)	Nimmo et al. (2007)
Ganymede	1.38*±0.02	1.84*±0.03	HE	Gomez Casajus et al. (2022)
Callisto	0.283*±0.004	0.377*±0.006	HE	Anderson et al. (2001)

shape act as a source of noise that could bias internal structure inference (Gao and Stevenson 2013). Spherical harmonic coefficients of gravity ($\bar{C}_{lm}$, $\bar{S}_{lm}$) and shape ($\bar{A}_{lm}$, $\bar{B}_{lm}$) can be expressed as a sum of hydrostatic and non-hydrostatic parts, denoted by superscripts "h" and "nh", respectively:

$$\{\bar{A}_{lm}, \bar{B}_{lm}\} = \{\bar{A}^h_{lm}, \bar{B}^h_{lm}\} + \{\bar{A}^{nh}_{lm}, \bar{B}^{nh}_{lm}\} \tag{7}$$

$$\{\bar{C}_{lm}, \bar{S}_{lm}\} = \{\bar{C}^h_{lm}, \bar{S}^h_{lm}\} + \{\bar{C}^{nh}_{lm}, \bar{S}^{nh}_{lm}\}. \tag{8}$$

The hydrostatic part can be computed using the Radau-Darwin relationship for a given moment of inertia (e.g., Dahlen and Tromp 1998) or using a more accurate theory of figures (Zharkov et al. 1985; Zharkov 2004; Zharkov and Karamurzov 2006; Zharkov and Gudkova 2010; Tricarico 2014) for a given density profile. Conversely, once the hydrostatic part (either in shape or in gravity) is isolated, these theories can then be used to directly recover the moment of inertia.

Iess et al. (2014) proposed that non-hydrostatic contributions to the shape and gravity degree-2 coefficients can be separated by assuming that the admittance depends on wavelength but not the spatial pattern of deformation. This isotropic assumption requires a constant ratio between the non-hydrostatic components of gravity and shape:

$$\frac{\bar{C}_{20}}{\bar{A}_{20}} = \frac{\bar{C}_{22}}{\bar{A}_{22}}. \tag{9}$$

Thus, with both degree-2 shape and gravity coefficients determined, it is possible to separate the hydrostatic and non-hydrostatic contributions by varying the internal structure model, and hence to determine the MoI. However, the gravity and shape coefficients need to be determined to a commensurate accuracy, which is challenging in the Jovian system as the current data were collected over a handful of flybys by *Voyager*, *Galileo* and *Juno*.

The ellipsoidal parameters for the Galilean moons are given in Table 2; for hydostatic bodies, the ratio $(a-b)/(a-c) = 3/4$, so this ratio provides a test of hydrostaticity. While Io is evidently close to hydrostatic, uncertainties in the shapes of the other bodies are too large to make any firm conclusions.

For Io, Europa and Ganymede, shape non-sphericity has been detected. However, the relatively low non-sphericity prevents use of the derived oblatenesses of Europa and Ganymede to study their interior. For example, the shape of Europa has been determined by fitting limb profiles and the uncertainty on the ellipsoidal axes is on the order of 0.3 km (Nimmo et al. 2007). This uncertainty corresponds to a moment of inertia uncertainty of ∼0.1. Therefore, the knowledge of Europa's shape is currently insufficient to meaningfully constrain Europa's interior. Ganymede's shape has been determined with and without enforcing hydrostaticity.

Zubarev et al. (2015) and Nadezhdina et al. (2024) developed a control point network (CPN) for Ganymede. However, if not constrained by hydrostatic equilibrium, their best-fit ellipsoids show surprisingly large non-sphericity (≈ 7 km). Therefore, Ganymede's shape needs to have an in-built assumption on the moment of inertia and cannot be used to constrain Ganymede's interior. Callisto's non-sphericity has not been detected (Anderson et al. 2001).

As discussed in Sect. 2.1, non-hydrostatic gravity ($l > 2$) has not been detected at Io or Europa, while Ganymede shows significant non-hydrostatic gravity anomalies at degree 3 to 5 (Gomez Casajus et al. 2022). For Callisto, the *Galileo* data has only been analyzed by enforcing the hydrostatic ratio $J_2/C_{22} = 10/3$, which led to the conclusion of a large moment of inertia and, therefore, an undifferentiated interior (Anderson et al. 2001) (see Sect. 2.6). However, due Callisto's slow rotation and large distance to Jupiter, the amplitude of the hydrostatic signal is small. Therefore, even a modest amount of non-hydrostaticity, such as due to presence of Valhalla basin, can bias the inferred moment of inertia (McKinnon 1997).

Having the shape expanded in spherical harmonics allows exploration in the spectral domain. The topographic Root-Mean-Square (RMS) spectrum can be found using spherical harmonic coefficients as:

$$M^{tt} = \left[\frac{\sum_{m=0}^{l} \bar{A}_{lm}^2 + \bar{B}_{lm}^2}{2l+1} \right]^{1/2} \tag{10}$$

$$M^{gg} = \left[\frac{\sum_{m=0}^{l} \bar{C}_{lm}^2 + \bar{S}_{lm}^2}{2l+1} \right]^{1/2}. \tag{11}$$

The gravity and topography RMS spectra depend on the mechanical strength of the body, i.e., the magnitude of non-hydrostatic stresses that can be supported over geological timescales. At high spherical harmonic degrees (short wavelengths), the RMS spectra of planetary shape can be well described by a power law (Meinesz 1950; Ermakov et al. 2018):

$$M^{tt} = kl^{\beta} \tag{12}$$

where k is the wavenumber and β is a constant. For low spherical harmonic degrees, where elastic stresses are not sufficient to support topography, the topographic power spectra have been observed to have a subdued power (Nimmo et al. 2011; Ermakov et al. 2018). The elastic support at low degrees depends on the thermal structure of the icy shells as warmer shells would yield more easily leading to more sudued topography (Conrad et al. 2021). This effect can be parametrized by introducing the effect of bending and membrane stresses in supporting topographic loads:

$$M^{tt} = kl^{\beta} \cdot F_l, \tag{13}$$

where $F_l = [(1 + (\rho_{shell}/\rho_{ocean} - \rho_{shell}) \cdot C_l]^{-1}$, C_l is the degree of compensation (Turcotte et al. 1981) that critically depends on the thickness of the elastic layer, and ρ_{shell} and ρ_{ocean} are the density of the shell and ocean. In the limit of C_l approaching zero, the resulting topography is equivalent to the load. Alternatively, in the limit of C_l approaching unity, the topography is supported solely by the buoyancy force (i.e., isostatically compensated). Thus, we can use RMS topographic spectra to constrain the thickness of the elastic layer, which is related to the thermal state of the outer shell. A low degree of support indicates a thin elastic layer, which means that the ice is warm and ductile at shallow depths, indicating a higher heat flux.

Another potential way of determining the degree of elastic support is to use gravity-topography admittance (Akiba et al. 2022). Unfortunately, at Europa the gravity signal from the rock-ocean interface is likely to dominate at long wavelengths (see below). As a result, gravity-admittance probes of the ice shell require high spatial resolution gravity fields to be successful (Koh et al. 2022). In any event, future measurements of gravity and shape of the Galilean moons can be used to provide independent constraints on the icy shell thermal structure.

Unlike for terrestrial worlds, it is possible that subsurface density interfaces contribute more to the gravity of Galilean moons than the surface. The density contrast between ice and vacuum is ≈ 900 kg/m^3, whereas the density contrast of the ocean-rock interface could reach 2000 kg/m^3. However, the gravity signal of the ocean bottom topography will be attenuated by an upward continuation factor $(r_{\text{ocean bottom}}/R_{\text{satellite}})^l$. Thus, it is possible that low spherical harmonic degrees in gravity will be dominated by the ocean floor topography signal (Pauer et al. 2010; Dombard and Sessa 2019; Koh et al. 2022). The power spectrum of the gravity signal can in principle be used to provide a constraint on the depth to the ocean floor (Cascioli et al. 2024), although this requires assumptions to be made about the power spectral slope of the ocean floor topography, which is unknown. If the ocean depth can be constrained via other means (e.g. induction), the gravity spectrum can then be used to derive the spectral properties of the ocean floor topography.

4.2 Tidal Response

Because of the moons' proximity to their large parent, their shapes are ellipsoidal rather than spherical — they have a permanent tidal bulge (see Sect. 4.1). Furthermore, because their orbits are not circular, the size and orientation of this bulge varies over the course of each orbit. This time-variable (diurnal) component of the tidal bulge is responsible for tidal heating of these bodies, and measurement of it can be used to place constraints on their internal structure.

The amplitude H of the diurnal tidal bulge is given by equation (3) and depends on the degree-two tidal Love number h_2 which provides a dimensionless measure of how deformable the satellite is. A measurement of h_2 provides constraints on the internal structure of a body: a fluid (strengthless), uniform body has $h_2 = 2.5$ and a more rigid or more centrally-condensed body has a lower h_2. For Europa, the amplitude H given by equation (3) is 23 m if $h_2 = 1$.

The surface deflections implied by equation (3) are generally small enough that to measure them requires a laser altimeter, such as that carried by *JUICE* (Kimura et al. 2019). Europa's surface deflection will be measured using radar altimetry (Steinbrügge et al. 2018), but the uncertainties are likely to be large.

Diurnal tides also involve periodic redistribution of mass, and thus a periodically varying gravity field. The amplitude of this variation is characterized by the tidal Love number k_2, where a uniform, strengthless body has a k_2 of 1.5. Measurement of k_2 can be obtained by spacecraft tracking and is thus easier to achieve than measurement of h_2. A combination of *Galileo* and *Juno* flybys have been used to deduce the k_2 of Io (Park et al. 2025a). *JUICE* and *Europa Clipper* will measure both k_2 and h_2 of Ganymede (Cappuccio et al. 2020; Steinbrügge et al. 2015) and Europa (Mazarico et al. 2023; Steinbrügge et al. 2018), respectively, with the accuracy of the former being several orders of magnitude better. *JUICE* will also assess the k_2 of Callisto, with much less accuracy, but still comparable to what was achieved at Titan by *Cassini* (Cappuccio et al. 2022).

For a purely elastic or completely inviscid body, the tidal response is exactly in phase with the tidal forcing. For real bodies, the tidal response will lag the forcing, and it is this

lag that gives rise to both tidal torques and tidal heating (Goldreich and Soter 1966). For a satellite, the lag angle is approximated by $1/2Q$ (Murray and Dermott 1999) where Q is the so-called dissipation factor, and a small Q means large dissipation. The tidal heating rate (equation (1)) is proportional to k_2/Q, which can also be written as $Im(k_2)$, where k_2 is now taken to be a complex quantity and is dependent on both the mechanical properties of the satellite and the forcing frequency. *JUICE* gravity measurements should be sufficiently accurate that the k_2/Q of Ganymede can be determined (Cappuccio et al. 2020). The gravity measurements performed at Callisto by *JUICE* will not be accurate enough to detect k_2/Q unless it is larger than 0.05-0.1, which seems unlikely; *Tianwen-4*, however, may be able to measure this quantity (Sun et al. 2026).

Apart from the degree 2 tide, the tidal force also contains shorter wavelength components that also produce tidal deformations. However, the amplitude of the tide quickly decays with degree l as $\propto (R/a)^l$, making it challenging to measure. Lateral heterogeneities within a moon (e.g., shell thickness variations, variations in shear modulus and viscosity) and ocean dynamics make it possible for the degree 2 tide to excite a response at $l > 2$ (A et al. 2014; Qin et al. 2016). Moreover, the tidal response also depends on the order m of the forcing. This challenges the traditional parametrization of the tidal response with a unique Love number per degree. To capture mode-coupling a more generalized version of Love numbers is needed: $k_{lm}^{l'm'}$, which indicate the tidal response at degree and order l' and m' due to a forcing at degree l and m. *Europa Clipper* will not be able to distinguish differences in the tidal response at different orders for Europa (Mazarico et al. 2023), but *JUICE* will. *JUICE* might be able to measure the different orders at degree 2, as well as potentially degrees $l > 2$ of the tidal response of Ganymede, as *GRAIL* did for the Moon (Williams et al. 2014). Due to the very high accuracy of 3GM gravity measurements, *JUICE* will also have the capability to detect any response to moon-moon tidal forcing (Hay et al. 2020) occurring at frequencies different from the main eccentricity tide (De Marchi et al. 2022).

4.2.1 Interpretation of k_2 and h_2

Once measurements of k_2, h_2 and potentially Q have been made, what can they tell us?

Presence of an Ocean The simplest use of Love numbers is to determine whether near-surface oceans are present. An ocean has no shear strength; by decoupling the shell from the deeper interior, it greatly reduces the ability of the shell to resist tidal stresses and as a result h_2 and k_2 are expected to be larger for ocean-bearing than ocean-free worlds (e.g. Moore and Schubert 2000, 2003).[5] The magnitude of the difference will be smaller for smaller bodies or for thicker shells (i.e. deeper oceans) (e.g. Goldreich and Mitchell 2010). Both amplitude and phase lag of the Love numbers are needed to confirm the presence of an ocean, as a very low viscosity, fully solid interior may result in high values of Love numbers comparable to models with an internal ocean (Moore and Schubert 2000, 2003; Kamata et al. 2016). At Io, a recent measurement of k_2 (Park et al. 2025a) has been used to rule out the presence of a shallow magma ocean (Sect. 2.3). The presence of an ocean would be confirmed by a low phase lag ($< 10^o$) and $k_2 > 0.2$ on Europa (Moore and Schubert 2000), or $k_2 > 0.3$ on Ganymede and Callisto (Moore and Schubert 2003; Kamata et al. 2016). To some extent, the combined amplitude and phase lag of k_2 and h_2 can be used to constrain the thickness and mechanical properties of the outer layer, as well as the density of the liquid layer (see below).

[5] Note that Love numbers do not *always* increase in the presence of an ocean; at Titan the reverse may be the case (Petricca et al. 2025b).

Shell Parameters (Thickness and Rigidity) Because the main role of the ocean is to act as a decoupling layer, the tidal response of an ocean-bearing body is not very sensitive to the ocean thickness (unless the ocean happens to be in a resonant configuration - see Sect. 3.2). It is, however, quite sensitive to the thickness and rigidity of the shell. In fact, it depends on the product of these two parameters; thus, by measuring Love numbers alone it is not possible to determine the thickness of the shell d unless the rigidity μ is known *a priori*. Measurement of a single Love number is also non-unique because of tradeoffs with ocean and shell density and mantle rigidity; measurement of both h_2 and k_2 reduces these tradeoffs but does not solve the $d - \mu$ tradeoff (Wahr et al. 2006). A shell with a sizeable low-viscosity layer (e.g. one that is convecting) would be expected to display a phase lag in its tidal response (e.g. Moore and Schubert 2000).

Ocean Characteristics Although not in general very sensitive to the ocean thickness, the tidal response of a body does care about the ocean density. In the absence of an overlying shell, the k_2 Love number is (e.g. Idini and Nimmo 2024)

$$k_2 = \frac{3}{5\frac{\bar{\rho}}{\rho} - 3}, \tag{14}$$

where $\bar{\rho}$ is the bulk density of the body and ρ the ocean density. A denser ocean enhances the tidal response. The presence of a rigid shell will suppress the response, but for the relatively thin-shell, large Galilean satellites this effect is relatively small (Goldreich and Mitchell 2010).

A perhaps more important characteristic of ocean layers is that they can exhibit inertial effects (sloshing) not present in solid layers. As a consequence, their tidal response can be more complicated, resulting in unexpected Love numbers. As explained in detail in Sect. 3.2, two cases are of particular interest.

First, in very thin (<1 km) oceans the gravity wave speed can equal the tidal forcing, leading to resonance. For obliquity tides, this resonance appears at much larger ocean thicknesses. Second, if the ocean is stably stratified, different combinations of thickness and stratification can lead to resonances with internal waves, and enhanced Love numbers (Idini and Nimmo 2024).

Deep Interior The decoupling effect of an ocean makes the tidal response relatively insensitive to the deep structure of a satellite. However, if the interior is sufficiently inviscid, then the *difference* between the phase lag as measured by k_2 and by h_2 is expected to exceed a few degrees (Hussmann et al. 2016). Measurements of this level of precision are expected at Ganymede with *JUICE* and Callisto with *Tianwen-4* (because these spacecraft are orbiters), but not at Europa.

3D Structure The effect of lateral heterogenities in the tidal response opens the door to using tidal tomography to constrain $3D$ structure (Qin et al. 2016; A et al. 2014; Berne et al. 2023; Rovira-Navarro et al. 2024). Tidal tomography requires very precise measurements of the tidal response, and therefore has only been applied to the Earth (Lau et al. 2017) and recently the Moon (Park et al. 2025b). *JUICE*'s orbital phase might provide the opportunity to use tidal tomography to constrain Ganymede's ice shell thickness variations (Rovira-Navarro et al. 2025). Measuring order differences in the degree two response would allow equator-to-pole shell thickness variations to be constrained, while additionally measuring the degree 3 response would allow detection of a North/South dichotomy and/or longitudinal shell thickness variations with a wavelength equal to or half the moon's circumference.

4.3 Rotation State

Readers interested in Galilean satellite rotation parameters are cautioned that the formal IAU values for these parameters are misleading, as they assume uniform rotation and zero obliquity, neither of which can be strictly correct (as explained below). Further discussion may be found in (Bills and Scott 2022; Yseboodt and Baland 2026) and (in the case of Europa) Steinbrügge et al. (2026).

4.3.1 Librations

The Galilean moons are thought to occupy a so-called Cassini state, i.e. a stable equilibrium rotation state in which their spin period is equal to their orbital period and the spin axis precesses together with the orbit normal maintaining a roughly constant and small angle (the obliquity) between them (Bills 2005). Equilibrium, however, does not imply a constant rotation rate since Jupiter exerts a gravitational torque on the moons as a result of (1) their triaxial ellipsoidal shape and (2) the deviation of their equatorial long axis from the direction to Jupiter. In the Newtonian two-body problem, for a low-eccentricity elliptical orbit, the moon's long axis is always directed to the empty focus of the orbit, and the largest deviation between the long axis and the direction to Jupiter is given by twice the eccentricity (e.g. Murray and Dermott 1999). Therefore, Jupiter exerts a periodic gravitational torque on the moons that is proportional to the orbital eccentricity and to the equatorial flattening of the moon. Knowledge of the resulting rotation variations, or longitudinal librations, is needed for cartography of the moons, but more importantly can give information on the interior of the moons.

If the moons were entirely solid and infinitely rigid, measurements of libration would allow determination of the equatorial flattening of the moon, given by the inertia ratio $(B - A)/C$, where A and B are the two principal equatorial moments of inertia and C the principal polar moment of inertia. Combined with measurements of the degree-two gravity field (C_{22} is proportional to $B - A$), libration could then in principle be used to determine each of the three principal moments of inertia independently. From those values, the mean moment of inertia can be determined, which is an essential quantity giving information on the radial density distribution in the moon (Sect. 2.1). The estimated libration amplitude for a solid and infinitely rigid Io, Europa, Ganymede and Callisto is about 270 m, 135 m, 10 m, and 12 m, respectively (Baland and Van Hoolst 2010), and can be measured with an orbiting spacecraft, such as *JUICE* for Ganymede (Van Hoolst et al. 2024), or through multiple spacecraft flybys, such as with *Clipper* for Europa (Roberts et al. 2023) and *JUICE* for Callisto (Van Hoolst et al. 2024).

The Galilean moons, however, are neither solid nor infinitely rigid. Subsurface oceans in Europa, Ganymede and Callisto and a magma ocean (if one exists) in Io would allow for differential rotation between the solid layers above and below. Although not equal, the librations of these two solid layers are coupled through a gravitational torque between them and through pressure couplings at the interfaces with the liquid layer. Viscous and electromagnetic torques are thought to have a negligible influence on the short period librations (Van Hoolst et al. 2008). A liquid subsurface layer can significantly increase the libration amplitude of the outer shell, in particular if it is thin. For Enceladus, the observed libration amplitude (Thomas et al. 2016) is about four times larger than the value of 135 m expected for an entirely solid and rigid moon. The large increase of the libration of the ice shell is mainly due to the moment of inertia of the shell being about five times smaller than that of the whole moon and to the fact that the torque on the shell from Saturn and the underlying

layers is about 2/3 of the total torque on the moon. The large observed libration amplitude is convincing proof that Enceladus has a global subsurface ocean. One might anticipate that a similar conclusion could be reached for the Galilean moons. For example, for a Europa with infinitely rigid solid layers, a subsurface ocean can increase the libration amplitude by up to 20 m (Van Hoolst et al. 2008), which can be measured. However, for satellites larger than Enceladus, the effect of the finite rigidity of the solid layers cannot be neglected and can even become dominant.

A moon with finite rigidity will deform in response to a changing potential, and this deformation can drastically change the librational response of a large moon. Deformation reduces the effective torque on the moon and its different internal layers (Van Hoolst et al. 2013) and therefore reduces libration; equally, this effect can be thought of as the result of elastic energy being required to deform the shell (Goldreich and Mitchell 2010). For large icy satellites, the crust almost deforms as a layer in hydrostatic equilibrium and its shape conforms to that of the response of the liquid layer beneath. This results in a small libration. Beuthe (2018) classified this tidal deformation behaviour as soft, whereas Enceladus's ice shell can be considered as hard. For example for Enceladus, the total torque on the ice shell is reduced by only $\simeq$3% with respect to an infinitely rigid moon. The effect is larger for the larger Galilean icy moons and can be up to 90% (Van Hoolst et al. 2013). The amplitude of the libration of the ice shell of Europa is therefore expected to be between about 70 m and 180 m, depending mainly on the ice shell thickness, rigidity and density (Van Hoolst et al. 2013). As a consequence, librations alone cannot be used to determine Europa's ice shell properties, although when combined with other measurements they are useful (Roberts et al. 2023). For example, adding libration constraints to Love number measurements can break the degeneracy between rigidity and shell thickness (Petricca et al. 2026).

The expected libration amplitudes of the ice shell of Ganymede and Callisto are within a few meters of the values for an entirely solid moon and depend only weakly on the properties of the ice shell (Van Hoolst et al. 2013). The libration of the solid interior beneath a liquid layer is slightly smaller than that of the shell for Europa, Ganymede and Callisto. Since it induces a time-dependent component in the degree-2 gravitational coefficients C_{22} and S_{22}, the interior libration can in principle be observed from radio-tracking gravity measurements (Van Hoolst et al. 2013).

Since Io is now not thought to have a magma ocean (Sect. 2.3), its libration amplitude is expected to be about 270 m (Van Hoolst et al. 2020). A measurement of Io's libration amplitude might thus provide a test of the inference that no magma ocean exists.

For a Galilean satellite in a Keplerian orbit, the gravitational torque from Jupiter not only excites a libration at orbital frequency but also at harmonics (integral multiples) of it. The amplitudes of those librations at the n-th harmonic frequency are a factor e^n smaller than the orbital libration. More interesting are librations due to deviations from a Keplerian orbit (Lainey et al. 2006), which perturb the gravitational torque exerted by Jupiter and lead to additional librations at the periods of the orbital perturbations, typically a few years (Henrard 2005). They are particularly relevant as a means to probe the moon's interior if their period is close to a libration eigenperiod (Rambaux et al. 2011). The periods of the libration eigenmodes are between 7.5 days and 61 days for Europa, between 63 days and 0.9 yr for Ganymede, and between 0.74 yr and 3.3 yr for Callisto (Van Hoolst et al. 2013). These can be close to orbital perturbation periods (Lainey et al. 2006); the Laplace resonance produces strong orbital fluctuations with periods in the range 462-485 days (Rambaux et al. 2011). The shells of the Galilean icy moons could also spin at a rate slightly below or above synchronous due to tidal or oceanic torques (Sect. 3.2). According to Ashkenazy et al. (2023) the differential rotation with respect to the synchronous rotation rate due to ocean

torques could exceed 30 m/yr (either prograde or retrograde) for Europa. Since the long-period librations can easily be distinguished from the diurnal libration, they are unlikely to affect the determination of the diurnal libration amplitude, but they could degrade any attempt to look for non-synchronous rotation.

4.3.2 Obliquity and Departure from Cassini State

In the Cassini state occupied by the Galilean moons, the obliquity cannot be zero because of orbital precession. If it were zero, the torque causing the precession of the moon would vanish and the moon's spin axis would not be able to follow the orbit normal, which is the requirement for a Cassini state (Bills 2005). The obliquity depends on how well the spin axis can track the motion of the orbit pole. For a spin precession much faster than the periods on which the orbit changes, obliquity is very small. For a spin precession period longer than the orbital precession, the spin axis would not be able to track the orbit normal, so the obliquity would be equal to the mean orbital inclination. Orbital precession occurs at different timescales, ranging from less than one year to several hundred years. The period of spin precession depends on the gravitational torque from Jupiter on the moon, and therefore depends on the interior structure of the moon (the degree-2 gravity moments) and tends to be smaller for shorter distances to the planet. For entirely solid moons, the spin precession period increases from 0.41 yr for Io to 203 yr for Callisto (Baland et al. 2012). Obliquity and the amplitude of oscillations in obliquity are therefore expected to be smallest for Io and largest for Callisto, with mean obliquities ranging from 0.002° for Io to about 0.15° for Callisto (Baland et al. 2012; Chen et al. 2014).

In the absence of a global internal liquid layer, measurements of the obliquity, as will be done by *JUICE* for Ganymede and *Tianwen-4* for Callisto in the early 2030s, together with the measurement of the degree-2 gravity field will help determine the mean moment of inertia of the moon (Bills 2005). With a global internal ocean, the situation becomes more complex and more interesting. Resonances can occur from proximity between spin precession periods and orbital precession periods, which can substantially increase the obliquity. Although resonances are also possible for an entirely solid Galilean moon, the interior structure with a global subsurface ocean offers more possibilities for resonances. The high obliquity of Titan was argued to be the consequence of such a resonance (Baland et al. 2011) or because of an ocean's decoupling effect (Bills and Nimmo 2011); more recent work, however, has attributed it to the large tidal response and concludes that an ocean is not present (Petricca et al. 2025b). In any event, detection of an ocean in the Galilean moons through obliquity measurements may be possible if the moon's internal structure leads to an obliquity measurably different from that expected for a solid moon.

The obliquity also offers insight into the interior structure, but direct determination of a specific interior property, such a shell thickness, is nontrivial since different interior structures can lead to about the same obliquity (Baland et al. 2012). However, whereas tides and libration are mainly determined by properties of the hydrosphere of the Galilean icy moons, obliquity also depends on the interior below the ocean. Joint inversion of these quantities can then be used to probe the deeper interior. In addition, obliquity can inform on dissipation processes in the moon's interior since it can lead to a small offset of the Cassini state from coplanarity (e.g. Williams et al. 2001 for the Moon, Baland et al. 2017 for Mercury, Downey and Nimmo 2025 for Titan). As an example, the projected uncertainty of *JUICE*'s measurement of Ganymede's obliquity (Cappuccio et al. 2020) should allow detection of k_2/Q as long as it exceeds 0.0016 (Downey and Nimmo 2025). Moreover, comparison of the obliquity of the ice shell, as observed by remote sensing instruments and the whole body

obliquity determined by gravity, can provide further information on the mass distribution and mechanical coupling.

4.4 Magnetic Measurements

Magnetic induction has been very successful at detecting high-conductivity layers at all four Galilean satellites (Sects. 2.3-2.6). However, current results are limited by the use of only a single forcing frequency. In this case, the technique is sensitive only to the product of conductivity and layer thickness, so that neither characteristic can be uniquely determined (Khurana et al. 2002). Furthermore, the induction response can saturate, so that (for instance) at Io it is not possible to use induction to distinguish between a partially-molten and a fully-molten mantle (Khurana et al. 2011).

In principle, both these obstacles can be overcome by measuring the induction response at multiple frequencies. Although the main forcing frequency is at Jupiter's synodic rotation period, there is also a signal at the orbital period, and both frequencies also have higher harmonics. A multi-frequency approach should be able to independently constrain the thickness and conductivity of a near-surface ocean (e.g. Biersteker et al. 2023). This approach is particularly powerful when combined with other techniques (e.g. Petricca et al. 2026), since (for instance) the tidal response (Sect. 4.2) depends on the thickness of the rigid part of the ice shell, while the induction response depends on the total thickness.

It would also be of interest to use magnetic induction to probe the deep interiors of these bodies, as has been done at the Moon (Hood et al. 1982). However, it seems likely that the induction signal of the shallow, highly conductive layer (the ocean or magma ocean) will swamp any signal from deeper conductive layers (Seufert et al. 2011). It thus appears that induction may be unsuitable for deep sounding, and that other techniques, such as precise rotational observations (cf. Williams et al. 2001) should be used instead.

The nature of Ganymede's internal dynamo is currently not well understood (Soderlund et al. 2025). *JUICE* will be able to characterize the spatial properties of the dynamo-generated field (Masters et al. 2025), and potentially look for any long-term variations in that field (such as the westwards drift of the terrestrial field).

4.5 Miscellaneous Measurements

Dissipation in Jupiter pushes the satellites outwards, but this effect is complicated by the Laplace resonance, and dissipation inside the moons (which moves them inwards). Nonetheless, with sufficiently good astrometric measurements of the satellites' orbital evolution, the k_2/Q of the moons can be obtained. To date, this has only been done for Io (Lainey et al. 2009). Future measurements by *Clipper*, *JUICE* or *Tianwen 4* will be able to use *Galileo*- or *Juno*-era observations, thus achieving a long time baseline.

For Io, a direct measurement of k_2/Q can be obtained based on the total heat output of about 10^{14} W (Veeder et al. 1994). Assuming that Io is in equilibrium, this heat output must be arising from tidal heating and therefore depends on k_2/Q (equation (1)). The value derived in this manner is consistent with those obtained from astrometry (Lainey et al. 2009) and from gravity measurements (Park et al. 2025a).

In principle, such measurements could be carried out at the other moons. The problem is that the tidal heat production is expected to be much lower, so the exogenic thermal output will be hard to distinguish from insolation. At Europa, exogenic heat sources might possibly be detectable near the poles using infra-red observations (Christensen et al. 2024), but not elsewhere. Rather than using infra-red measurements, an alternative is to use a microwave

radiometer, which can in principle detect thermal gradients in the ice shell (Brown et al. 2023; Levin et al. 2026). The problem here is that the presence of fractures or small amounts of a conductive contaminant can change the microwave response of the shell, making the problem highly non-unique.

One potentially powerful probe of the shallow subsurface is an ice-penetrating radar, as carried by both *JUICE* and *Clipper*. The detailed structure of the near-surface ice, including layering, fractures and intruded bodies of water, if any, should be clearly visible (Blankenship et al. 2024). It is less likely, however, that the radar will be able to detect the ice-ocean interface. The problem is that ice near the melting point is very dissipative at radar frequencies (Moore 2000), so any returned signal will be so strongly attenuated as to be invisible. Nonetheless, these radar instruments will at least be able to place a strong lower bound on the potential ice shell thickness. Undulations in the depth to this attenuating layer would be indicative of lateral variations in the temperature structure, signaling either convective upwellings/downwellings or variations in the conductive shell thickness. Either result would be very interesting, and the two inferences could in principle be distinguished by also measuring the surface topography.

An important aspect of both *Clipper* and *JUICE*'s investigations is the joint analysis of multiple data sets (Roberts et al. 2023; Van Hoolst et al. 2024; Petricca et al. 2026). Thus, for instance, induction sounding, tidal response measurements and radar can be combined to determine Europa's ice shell thickness. Similarly, Ganymede's librations will be measured both optically and by gravity, and a difference in the two measurements would provide additional information about its internal structure and dynamics. The same comment applies to measurements of k_2/Q via gravity and rotation state measurements.

Finally, many of the spacecraft measurements described above can be complemented by laboratory measurements. Although a lot of effort has been expended in determining likely ocean electrical conductivities (e.g. Castillo-Rogez et al. 2022), the conductivity of ice (and especially contaminated ice) at low temperatures is not currently well-characterized. The dissipative behaviour of ice and rock, especially in the presence of partial melt, is also not yet well understood (e.g. Takei 2017).

5 Outstanding Questions

Having surveyed our existing knowledge in Sects. 2 and 3, we will now summarize some of the most important open questions that remain.

1. Is Callisto differentiated? As explained in Sect. 2.6, the conclusion that Callisto is incompletely differentiated is based on an assumption of hydrostatic equilibrium which is not known to be correct. The reason that this question is so important is that avoiding ice-rock differentiation places stringent constraints on how Callisto could have accreted (e.g. Barr and Canup 2008). This issue is discussed in more detail in Nimmo et al. (2026) but, in brief, a partially-differentiated Callisto would require both slow accretion and an absence of giant impacts.

2. Does Europa have an iron core? Existing moment of inertia determinations for Europa are rather uncertain, but hint at a small (or even absent) core (Sect. 2.4). However, the non-uniqueness of an MoI constraint precludes a definitive conclusion. If a separate core does not exist, then that would place quite strong constraints on the body's thermal evolution (Trinh et al. 2023; Petricca et al. 2025a) and likely rule out strong tidal heating in Europa's mantle.

3. Are there oceans on Callisto and Io? At Callisto, the existence of a thick ionosphere has complicated investigations of whether it has a subsurface ocean or not (Sect. 2.6). Given Callisto's undeformed surface and (perhaps) incompletely-differentiated interior, an ocean is slightly surprising (but is certainly not ruled out). Meanwhile, a recent measurement of k_2 at Io is interpreted as ruling out a shallow magma ocean (Sect. 2.3). This conclusion is consistent with the available magnetic data, but has not yet been confirmed by another observation (e.g. librations). The absence of a magma ocean can be explained by rapid upwards migration and eruption of melt, but has important implications for the likelihood of magma oceans elsewhere (such as close-in exoplanets).

4. What is the magnitude and spatial distribution of tidal heating on Io, Europa and Ganymede? At Io, two independent measurements of k_2/Q (from gravity and heat flow) provide a good constraint on the present-day heat production rate (Sect. 2.3). However, it is not yet clear whether the heating is concentrated more towards the equator or the poles (e.g. Zambon et al. 2023; Davies et al. 2024). The pattern is important because it tells us whether the tidal heating is more pronounced towards the surface or at depth, respectively (Ross et al. 1990). For Europa, no measurements of tidal heating exist. Although it is generally assumed that heating is concentrated in the ice shell, there is no *a priori* reason that the mantle should not be warm and dissipative. Ganymede's low eccentricity and large distance suggest that tidal heating should not be significant at the present day; there are no current constraints on how much heating is happening, or where it is located.

5. What is the thickness of Europa and Ganymede's ice shells, and what are their structure and dynamics? Europa and Ganymede's shell thicknesses, structure and dynamics are currently very uncertain (Roberts et al. 2023; Vance et al. 2014; Van Hoolst et al. 2024). A shell thickness measurement would significantly improve our understanding of either body's thermal energy budget. The shells may undergo lateral flow, smoothing out topography, and they may also be undergoing convection (Sect. 3.1) - but observations are lacking. Lenses of water might be present in the ices of both moons. Melt pockets might be present in Ganymede's high pressure ice layer (Kalousová et al. 2018) and their presence in Europa's outer shell could be responsible for circular surface features (Manga and Michaut 2017). For Europa, there have been claims for eruptive plumes similar to those seen at Enceladus (Roth et al. 2014), but the evidence is weak (Roth et al. 2026).

6. What are the depths, composition and dynamics of subsurface oceans? As explained in Sect. 4.4, single-frequency magnetic induction sounding has significant limitations. We do not know the depth of any of the inferred oceans, and while we know they are at least somewhat conductive, there is little direct compositional information (except for surface spectra; Sect. 2.1). The dynamics of these oceans are even more poorly constrained (Sect. 3.2) and depend on unknown parameters such as the degree (if any) of ocean stratification, the basal heat flux and the roughness of the seafloor topography.

7. What is driving Ganymede's dynamo? The existence of a dynamo at Ganymede, and the absence of one at Io and Europa, is puzzling. Most workers assume that the dynamo is driven primarily by compositional buoyancy (e.g. Hauck et al. 2006) but the details are not well understood. As one of only a handful of active dynamos, a better characterization of this example would help understand the presence (or absence) of dynamos elsewhere.

6 How Well Will *Juno*, *JUICE*, *Clipper* and *Tianwen-4* Address These Questions?

1. Is Callisto differentiated? This question seems very likely to be answered. As summarized in Sect. 4.2, *JUICE* will carry out about 20 close flybys of Callisto which will

be enough to thoroughly characterize the degree-2 gravity field and determine the non-hydrostatic component (if any). Additional flybys by *Europa Clipper* and follow-up measurements by *Tianwen-4* will also help.

2. Does Europa have an iron core? While *Clipper* will improve Europa's low-degree gravity field measurements and hence MoI determination, the non-uniqueness problem will remain. If the total hydrosphere thickness can be constrained from magnetic induction measurements, the gravity data interpretation will provide less ambiguous solution on the deep interior structure. As discussed in Sect. 4.4, induction sounding is unlikely to be useful as a probe of deep interior structure; high-precision measurements of rotation state, however, might provide a constraint.

3. Are there oceans on Callisto and Io? As with Q1, the number of close flybys by *JUICE*, possibly complemented by flybys of *Clipper*, and later *Tianwen-4*, will be sufficient to comprehensively answer this question for Callisto using induction measurements. At Io, confirmation of the absence of a magma ocean would most readily be answered by a libration measurement (Sect. 4.3.1). This would most likely require a future spacecraft mission, though in principle ground-based techniques could also be used (Margot et al. 2013).

4. What is the magnitude and spatial distribution of tidal heating on Io, Europa and Ganymede? At Io, further analysis of existing *Juno* heat flow data seems likely to answer this question. At Europa, the situation is less clear-cut. A direct (gravity) measurement of k_2/Q at Europa is challenging, unless if Q is very low (< 10), and surface heat flow probably won't be large enough to be detectable, except in some local hotspots. Shell thickness variations might be interpreted as arising from tidal heating variations, but the ocean and/or lateral shell flow may provide confounding effects (Sect. 3.2), and whether the heating is located in the mantle or the ice shell will be hard to determine. Radar profiles of the ice shell, particularly when combined with MWR measurements (e.g. Levin et al. 2026), may provide estimates of local thermal gradients and thus heat flux variations. Although radar is unlikely to image the base of the shell (Sect. 4.5), a comparison of shell thickness bounds from radar with shell thickness measurements (e.g. from induction) might allow the thickness of a basal, tidally-heated layer to be determined. At Ganymede, present-day tidal heating is expected to be small enough compared to radiogenic heating that measuring heat flow anomalies is very unlikely. However, due to very high accuracy of the gravity measurements, *JUICE* will be able to quantify the imaginary part of k_2 with a stated accuracy of 6.8×10^{-5} (Cappuccio et al. 2020), thus providing key constraints on the dissipative processes and viscosity structure of the interior.

5. What is the thickness of Europa, Ganymede and Callisto's ice shells, and what are their structure and dynamics? A combination of induction measurements, radar sounding and k_2, h_2 and long-wavelength gravity-topography measurements should provide reasonable constraints on Europa's shell thickness (Roberts et al. 2023). Radar sounding should certainly be able to identify hypothesized near-surface regions of liquid water. A large mismatch between the radar penetration depth and the total ice shell thickness would be indicative of a convecting ice shell. Plumes, or plume deposits, should be detectable by multiple instruments - if they exist. Similar constraints, albeit with more precision, will be available at Ganymede thanks to *JUICE*, which will orbit at low altitude (≤ 500 km) during at least 3 months (Van Hoolst et al. 2024). *JUICE* and *Tianwen-4* will also provide geodetic data (e.g. spin pole orientation and librations; Sect. 4.3.2) of a kind unavailable at Europa, that may further sharpen our picture of Ganymede's and Callisto's interiors. *Clipper* and *JUICE* will not provide short-wavelength gravity and topography data suitable for constraining Callisto's ice shell thickness and possible lateral variations, but *Tianwen-4* will, being capable of measuring the gravity field at $\sim$200 km resolution (Sun et al. 2026).

6. What are the depths, composition and dynamics of subsurface oceans? Multi-frequency induction sounding (Sect. 4.4) should provide good constraints on both the thicknesses and the conductivities of the oceans at Europa, Ganymede and (with *Tianwen-4*) Callisto. Converting from conductivity to composition is not straightforward, but will be aided by much-improved surface composition measurements. Ocean dynamics, on the other hand, are hard to determine. At Europa, shell thickness variations might help, but are complicated to interpret (Sect. 3.2). Such variations will not arise at Callisto or Ganymede (the ice will flow laterally). Non-synchronous rotation could provide another constraint (Sect. 3.2). Mean ocean flows would generate a separate induction signal that could in principle be measured, as has been done for Earth (Tyler et al. 2003), but the detection of such signals is very challenging as the expected magnitude at Europa is very weak (< 1 nT) (Šachl et al. 2025). Detecting such a signal with orbiters - *JUICE* at Ganymede and *Tianwen-4* at Callisto - appears more promising but still challenging.

7. What is driving Ganymede's dynamo? As an orbiter, *JUICE* should provide excellent characterization of Ganymede's dynamo. In particular, the slope of the magnetic power spectrum should yield a depth to the top of the core (as is the case for Earth). More speculatively, the magnetic field might exhibit secular drift, which would provide constraints on the mean flow speed and thus the energy driving the flow. These measurements would provide at least partial answers to the question.

7 What High-Priority Questions Will Not Be Answered, and What Are the Key Future Measurements?

Questions 1, 3 and 5 are likely to be answered by *Juno* and/or the forthcoming *JUICE*, *Europa Clipper* and *Tianwen-4* missions. Question 4 (tidal heating) is likely to be harder to answer, except for Io. For Ganymede, the effects are expected to be small, though obliquity measurements may constrain k_2/Q. At Europa the effects may be larger but *Clipper* measurements may not yield a definitive answer. Question 2 (Europa core) likewise may be hard to answer with *Clipper* data. It is hard to imagine how Question 7 (Ganymede dynamo) could be answered definitively, although a determination of core size will yield a sulphur concentration and thus clarify potential mechanisms somewhat. Question 6 (oceans) is in some ways the most interesting question, because of its novelty (ocean dynamics of icy worlds is a new field) and its connections to astrobiology. Determining ocean thicknesses and conductivities are key aims of both *JUICE* and *Clipper*. Inferring ocean dynamics, however, is much harder: there are few observables that can be tied to ocean dynamics, and those that do exist are often affected by other processes as well. This is not really a problem with the available or anticipated measurements so much as a fundamental limitation imposed by non-uniqueness and confounding factors.

Current strategic exploration plans for both NASA and ESA envisage a likely shift from the Galilean satellites to Enceladus after *JUICE/Clipper* have completed their missions. Nonetheless, it is of interest to speculate what follow-on missions might look like. At Europa, a surface lander (Hand et al. 2022) would seem the obvious next step, especially if recent or current activity is detected, while a landed element may form part of the *Tianwen-4* mission. From the Interiors perspective, radio tracking of a lander to derive rotation state and surface deformation, and seismology to probe the structure of the ice shell ocean, and deep interior (e.g. Panning et al. 2006), and also assess the level of geologic activity, would be particularly valuable. A Europa Orbiter (e.g. Prockter et al. 2011) would be hampered

by the expected short lifetime due to radiation damage, but would provide *JUICE*-like measurements of gravity, topography, tidal response, induction and rotation state. In the post-*JUICE/Clipper* era, the least well-understood moon will be Io. Although *Juno* has provided important new information, the conclusion that Io lacks a global magma ocean is sufficiently surprising that confirmation (e.g. via libration measurements) would be desirable, as would a more precise set of induction measurements; such observations probably require a dedicated spacecraft. Remote sensing of isotopic data by ALMA (de Kleer et al. 2024) will probably continue to yield new information, but for transformative measurements, an Io sample return mission could be envisaged (Ogliore et al. 2024).

8 Summary and Conclusions

Most of our current knowledge of the interiors of the Galilean satellites comes from static or time-variable gravity data, and from magnetic induction studies. This is largely a reflection of the fact that *Galileo* and *Juno* were both satellite flyby missions. Despite their limitations, we have learned that all three icy moons likely possess subsurface oceans, while conversely Io lacks a magma ocean. Callisto's differentiation state remains an open question, as does the thickness of Europa's ice shell, the state and size of its core, and the distribution and magnitude of tidal heating on the three inner bodies. The dynamics of the subsurface oceans have attracted a great deal of theoretical attention, but connecting ocean processes to observable quantities such as non-synchronous rotation is challenging.

Forthcoming missions (*JUICE, Clipper* and *Tianwen-4*) will provide observations, such as radar sounding, thermal and mass spectrographic measurements, of a kind not available hitherto. Furthermore *JUICE* will orbit Ganymede - the first orbiter of an outer solar system moon — and will thus provide very high precision geodetic measurements. It is tempting to speculate as to what new discoveries these new instruments will make. As the more active of the three outer moons, it seems plausible that thermal anomalies similar to those seen at Enceladus will be observed at Europa. Ocean dynamics, however, are more likely to be detected at Ganymede, most likely through a combination of rotation state measurements and (perhaps) induction studies. Tidal measurements will give a better picture of the states of the bodies' mantles (are they hot or cold?). And the question of the degree to which Callisto is differentiated will surely be resolved.

Ultimately, of course, a major aim of all three missions is to determine how habitable these ocean worlds are. Unless there is active venting of material (which seems unlikely), direct measurements of ocean composition — as at Enceladus — may not be possible. But the planned observations will not only vastly improve our knowledge of the subsurface structure, they will also open up new avenues to understanding the long-term histories of these bodies, a key aspect of habitability. Those histories, in turn, will help us understand how the moons formed in the first place. As reviewed in Nimmo et al. (2026), doing so will not be straightforward. But it will provide intellectual challenges aplenty for the next generation of outer solar system scientists.

Acknowledgements FN acknowledges partial support from the Europa Clipper project. TVH acknowledges support from the Belgian PRODEX program managed by the European Space Agency in collaboration with the Belgian Federal Science Policy Office. GT acknowledges support from CNES for his participation to the JUICE and Europa Clipper mission. AE was partially supported by NASA's Juno Participating Scientist Program and the Precursor Science Investigation for Europa program.

Declarations

Competing Interests The authors declare that they have no conflict of interest.

Open Access This article is licensed under a Creative Commons Attribution 4.0 International License, which permits use, sharing, adaptation, distribution and reproduction in any medium or format, as long as you give appropriate credit to the original author(s) and the source, provide a link to the Creative Commons licence, and indicate if changes were made. The images or other third party material in this article are included in the article's Creative Commons licence, unless indicated otherwise in a credit line to the material. If material is not included in the article's Creative Commons licence and your intended use is not permitted by statutory regulation or exceeds the permitted use, you will need to obtain permission directly from the copyright holder. To view a copy of this licence, visit http://creativecommons.org/licenses/by/4.0/.

References

A G, Wahr J, Zhong S (2014) The effects of laterally varying icy shell structure on the tidal response of Ganymede and Europa. J Geophys Res 119(3):659–678
Akiba R, Ermakov AI, Militzer B (2022) Probing the icy shell structure of ocean worlds with gravity–topography admittance. Planet Sci J 3(3):53
Amit H, Choblet G, Tobie G, et al (2020) Cooling patterns in rotating thin spherical shells — application to Titan's subsurface ocean. Icarus 338:113509
Anderson J, Jacobson R, McElrath T, et al (2001) Shape, mean radius, gravity field, and interior structure of Callisto. Icarus 153(1):157–161
Ashkenazy Y, Tziperman E (2021) Dynamic Europa ocean shows transient Taylor columns and convection driven by ice melting and salinity. Nat Commun 12(1):1–12
Ashkenazy Y, Tziperman E, Nimmo F (2023) Non-synchronous rotation on Europa driven by ocean currents. AGU Adv 4(3):e2022AV000849
Aurnou J, Heimpel M, Wicht J (2007) The effects of vigorous mixing in a convective model of zonal flow on the ice giants. Icarus 190(1):110–126
Baland RM, Van Hoolst T (2010) Librations of the Galilean satellites: the influence of global internal liquid layers. Icarus 209(2):651–664
Baland RM, Van Hoolst T, Yseboodt M, et al (2011) Titan's obliquity as evidence of a subsurface ocean? Astron Astrophys 530:A141
Baland RM, Yseboodt M, Van Hoolst T (2012) Obliquity of the Galilean satellites: the influence of a global internal liquid layer. Icarus 220(2):435–448
Baland RM, Yseboodt M, Rivoldini A, et al (2017) Obliquity of Mercury: influence of the precession of the pericenter and of tides. Icarus 291:136–159
Barr AC, Canup RM (2008) Constraints on gas giant satellite formation from the interior states of partially differentiated satellites. Icarus 198(1):163–177
Berne A, Simons M, Keane JT, et al (2023) Inferring the mean thickness of the outer ice shell of Enceladus from diurnal crustal deformation. J Geophys Res Planets 128(6):e2022JE007712
Beuthe M (2016) Crustal control of dissipative ocean tides in Enceladus and other icy moons. Icarus 280:278–299
Beuthe M (2018) Enceladus's crust as a non-uniform thin shell: I tidal deformations. Icarus 302:145–174
Bierson C, Nimmo F (2016) A test for Io's magma ocean: modeling tidal dissipation with a partially Molten mantle. J Geophys Res Planets 121(11):2211–2224
Biersteker JB, Weiss BP, Cochrane CJ, et al (2023) Revealing the interior structure of icy moons with a Bayesian approach to magnetic induction measurements. Planet Sci J 4(4):62
Bills BG (2005) Free and forced obliquities of the Galilean satellites of Jupiter. Icarus 175(1):233–247
Bills BG, Nimmo F (2011) Rotational dynamics and internal structure of Titan. Icarus 214(1):351–355
Bills BG, Scott BR (2022) Rotation models for the Galilean satellites. Planet Space Sci 219:105474
Bire S, Kang W, Ramadhan A, et al (2022) Exploring ocean circulation on icy moons heated from below. J Geophys Res Planets 127:e2021JE007025
Blankenship DD, Moussessian A, Chapin E, et al (2024) Radar for Europa assessment and sounding: ocean to near-surface (REASON). Space Sci Rev 220(5):51
Brown S, Zhang Z, Bolton S, et al (2023) Microwave observations of Ganymede's sub-surface ice: I. Ice temperature and structure. J Geophys Res Planets 128(6):e2022JE007609
Busse FH (1970) Thermal instabilities in rapidly rotating systems. J Fluid Mech 44(3):441–460
Cappuccio P, Hickey A, Durante D, et al (2020) Ganymede's gravity, tides and rotational state from JUICE's 3GM experiment simulation. Planet Space Sci 187:104902
Cappuccio P, Di Benedetto M, Durante D, et al (2022) Callisto and Europa gravity measurements from JUICE 3GM experiment simulation. Planet Sci J 3(8):199

Carlson RW, Calvin WM, Dalton JB, et al (2009) Europa's surface composition. In: Pappalardo RT, McKinnon WB, Khurana KK (eds) Europa, p 283
Casajus LG, Zannoni M, Modenini D, et al (2021) Updated Europa gravity field and interior structure from a reanalysis of Galileo tracking data. Icarus 358:114187
Cascioli G, Mazarico E, Dombard A, et al (2024) Leveraging the gravity field spectrum for icy satellite interior structure determination: the case of Europa with the Europa Clipper Mission. Planet Sci J 5(2):45
Castillo-Rogez J, Daswani M, Glein C, et al (2022) Contribution of non-water ices to salinity and electrical conductivity in ocean worlds. Geophys Res Lett 49(16):e2021GL097256
Cebron D, Le Bars M, Moutou C, et al (2012) Elliptical instability in terrestrial planets and moons. Astron Astrophys 539:A78
Chen E, Nimmo F, Glatzmaier GA (2014) Tidal heating in icy satellite oceans. Icarus 229:11–30
Choblet G, Tobie G, Sotin C, et al (2017) Powering prolonged hydrothermal activity inside Enceladus. Nat Astron 1(12):841–847
Christensen PR, Spencer JR, Mehall GL, et al (2024) The Europa Thermal Emission Imaging System (E-THEMIS) investigation for the Europa Clipper Mission. Space Sci Rev 220:38
Cochrane CJ, Vance SD, Castillo-Rogez JC, et al (2025) Stronger evidence of a subsurface ocean within Callisto from a multifrequency investigation of its induced magnetic field. AGU Adv 6(1):e2024AV001237
Collins GC, McKinnon WB, Moore JM, et al (2009) Tectonics of the outer planet satellites. Planet Tecton 11(264):229
Conrad J, Nimmo F, Beyer R, et al (2021) Heat flux constraints from variance spectra of Pluto and Charon using limb profile topography. J Geophys Res Planets 126(2):e2020JE006641
Crawford GD, Stevenson DJ (1988) Gas-driven water volcanism and the resurfacing of Europa. Icarus 73(1):66–79
Dahlen F, Tromp J (1998) Theoretical global seismology. Princeton University Press
Davies M, Colvin T, Oberst J, et al (1998) The control networks of the Galilean satellites and implications for global shape. Icarus 135(1):372–376
Davies AG, Perry JE, Williams DA, et al (2024) Io's polar volcanic thermal emission indicative of magma ocean and shallow tidal heating models. Nat Astron 8(1):94–100
de Kleer K, Hughes EC, Nimmo F, et al (2024) Isotopic evidence of long-lived volcanism on Io. Science 384(6696):682–687
De Marchi F, Cappuccio P, Mitri G, et al (2022) Frequency-dependent Ganymede's tidal Love number k2 detection by JUICE's 3GM experiment and implications for the subsurface ocean thickness. Icarus 386:115150
Dombard AJ, McKinnon WB (2006) Elastoviscoplastic relaxation of impact crater topography with application to Ganymede and Callisto. J Geophys Res Planets 111(E1)
Dombard AJ, Sessa AM (2019) Gravity measurements are key in addressing the habitability of a subsurface ocean in Jupiter's Moon Europa. Icarus 325:31–38
Downey BG, Nimmo F (2025) Titan's spin state as a constraint on tidal dissipation. Sci Adv 11(6):eadl4741
Durham WB, Prieto-Ballesteros O, Goldsby D, et al (2010) Rheological and thermal properties of icy materials. Space Sci Rev 153:273–298
Ermakov A, Park R, Bills B (2018) Power laws of topography and gravity spectra of the Solar System bodies. J Geophys Res Planets 123(8):2038–2064
Gao P, Stevenson DJ (2013) Nonhydrostatic effects and the determination of icy satellites' moment of inertia. Icarus 226(2):1185–1191
Garrett C, Kunze E (2007) Internal tide generation in the deep ocean. Annu Rev Fluid Mech 39(1):57–87
Gastine T, Aurnou JM (2023) Latitudinal regionalization of rotating spherical shell convection. J Fluid Mech 954:R1
Gastine T, Favier B (2024) Rotating convection with a melting boundary: an application to the icy moons. Icarus, 116441
Gastine T, Wicht J, Aubert J (2016) Scaling regimes in spherical shell rotating convection. J Fluid Mech 808:690–732
Goldreich PM, Mitchell JL (2010) Elastic ice shells of synchronous moons: implications for cracks on Europa and non-synchronous rotation of Titan. Icarus 209(2):631–638
Goldreich P, Soter S (1966) Q in the Solar System. Icarus 5(1–6):375–389
Goldsby DL, Kohlstedt DL (2001) Superplastic deformation of ice: experimental observations. J Geophys Res, Atmos 106(B6):11017–11030
Gomez Casajus L, Ermakov A, Zannoni M, et al (2022) Gravity field of Ganymede after the Juno extended mission. Geophys Res Lett 49(24):e2022GL099475
Greeley R, Klemaszewski J, Wagner R, et al (2000) Galileo views of the geology of Callisto. Planet Space Sci 48(9):829–853
Greenberg R, Weidenschilling SJ (1984) How fast do Galilean satellites spin? Icarus 58(2):186–196

Hand KP, Phillips CB, Murray A, et al (2022) Science goals and mission architecture of the Europa Lander Mission concept. Planet Sci J 3(1):22
Hartkorn O, Saur J (2017) Induction signals from Callisto's ionosphere and their implications on a possible subsurface ocean. J Geophys Res Space Phys 122(11):11–677
Hauck SA, Aurnou JM, Dombard AJ (2006) Sulfur's impact on core evolution and magnetic field generation on Ganymede. J Geophys Res Planets 111(E9)
Hay HCFC, Trinh A, Matsuyama I (2020) Powering the Galilean satellites with moon-moon tides. Geophys Res Lett 47(15):e2020GL088317
Hay H, Fenty I, Pappalardo R, et al (2023) Turbulent drag at the ice-ocean interface of Europa in simulations of rotating convection: implications for nonsynchronous rotation of the ice shell. J Geophys Res Planets 128(3):e2022JE007648
Hay HC, Hewitt I, Katz RF (2024) Tidal forcing in icy-satellite oceans drives mean circulation and ice-shell torques. J Geophys Res Planets 129(6):e2024JE008408
Henrard J (2005) Additions to the theory of the rotation of Europa. Celest Mech Dyn Astron 93:101–112
Hood L, Herbert F, Sonett C (1982) The deep lunar electrical conductivity profile: structural and thermal inferences. J Geophys Res, Solid Earth 87(B7):5311–5326
Hoppa G, Tufts BR, Greenberg R, et al (1999a) Strike–slip faults on Europa: global shear patterns driven by tidal stress. Icarus 141(2):287–298
Hoppa GV, Tufts BR, Greenberg R, et al (1999b) Formation of cycloidal features on Europa. Science 285(5435):1899–1902
Hussmann H, Shoji D, Steinbrügge G, et al (2016) Constraints on dissipation in the deep interiors of Ganymede and Europa from tidal phase-lags. Celest Mech Dyn Astron 126:131–144
Idini B, Nimmo F (2024) Resonant stratification in Titan's global ocean. Planet Sci J 5(1):15
Iess L, Stevenson DJ, Parisi M, et al (2014) The gravity field and interior structure of Enceladus. Science 344(6179):78–80
Jansen MF, Kang W, Kite ES, et al (2023) Energetic constraints on ocean circulations of icy ocean worlds. Planet Sci J 4(6):117
Journaux B, Brown JM, Pakhomova A, et al (2020) Holistic approach for studying planetary hydrospheres: Gibbs representation of ices thermodynamics, elasticity, and the water phase diagram to 2300 MPa. J Geophys Res Planets 125(1):e2019JE006176
Kalousová K, Sotin C, Choblet G, et al (2018) Two-phase convection in Ganymede's high-pressure ice layer — implications for its geological evolution. Icarus 299:133–147
Kamata S, Kimura J, Matsumoto K, et al (2016) Tidal deformation of Ganymede: sensitivity of Love numbers on the interior structure. J Geophys Res Planets 121(7):1362–1375
Kang W (2022) Different ice-shell geometries on Europa and Enceladus due to their different sizes: impacts of ocean heat transport. Astrophys J 934(2):116
Kang W (2023) The modulation effect of ice thickness variations on convection in icy ocean worlds. Mon Not R Astron Soc 525(4):5251–5261
Kang W (2024) Nonsynchronous rotation of icy moon ice shells: the thermal wind perspective. Sci Adv 10(4):eadk2277
Kang W, Jansen M (2022) On icy ocean worlds, size controls ice shell geometry. Astrophys J 935(2):103
Kang W, Mittal T, Bire S, et al (2022) How does salinity shape ocean circulation and ice geometry on Enceladus and other icy satellites? Sci Adv 8(29):eabm4665
Kerswell RR (2002) Elliptical instability. Annu Rev Fluid Mech 34:83–113
Khurana KK, Kivelson MG, Russell CT (2002) Searching for liquid water in Europa by using surface observatories. Astrobiology 2(1):93–103
Khurana KK, Jia X, Kivelson MG, et al (2011) Evidence of a global magma ocean in Io's interior. Science 332(6034):1186–1189
Kimura J, Hussmann H, Kamata S, et al (2019) Science objectives of the Ganymede Laser Altimeter (GALA) for the JUICE mission. Trans Jpn Soc Aeronaut Space Sci Aerosp Technol Jpn 17(2):234–243
Kivelson M, Khurana K, Volwerk M (2002) The permanent and inductive magnetic moments of Ganymede. Icarus 157(2):507–522
Koh ZW, Nimmo F, Lunine JI, et al (2022) Assessing the detectability of Europa's seafloor topography from Europa Clipper's gravity data. Planet Sci J 3(8):197
Kvorka J, Čadek O (2022) A numerical model of convective heat transfer in Titan's subsurface ocean. Icarus 376:114853
Kvorka J, Čadek O (2024) The role of subsurface ocean dynamics and phase transitions in forming the topography of icy moons. Icarus 412:115985
Kvorka J, Čadek O, Tobie G, et al (2018) Does Titan's long-wavelength topography contain information about subsurface ocean dynamics? Icarus 310:149–164

Lainey V, Duriez L, Vienne A (2006) Synthetic representation of the Galilean satellites' orbital motions from L1 ephemerides. Astron Astrophys 456(2):783–788
Lainey V, Arlot JE, Karatekin Ö, et al (2009) Strong tidal dissipation in Io and Jupiter from astrometric observations. Nature 459(7249):957–959
Lau HCP, Mitrovica JX, Davis JL, et al (2017) Tidal tomography constrains Earth's deep-mantle buoyancy. Nature 551(7680):321–326
Le Bars M, Cébron D, Le Gal P (2015) Flows driven by libration, precession, and tides. Annu Rev Fluid Mech 47:163–193
Lemasquerier D, Grannan AM, Vidal J, et al (2017) Libration-driven flows in ellipsoidal shells. J Geophys Res Planets 122(9):1926–1950
Lemasquerier D, Bierson CJ, Soderlund KM (2022) Can convection in icy moons' oceans translate interior tidal heating patterns to the ice-ocean boundary? In: AGU Fall Meeting
Levin S, Zhang Z, Bolton S, et al (2026) Europa's ice thickness and subsurface structure characterized by the Juno microwave radiometer. Nat Astron 10:84–91
Lobo AH, Thompson AF, Vance SD, et al (2021) A pole-to-equator ocean overturning circulation on Enceladus. Nat Geosci 14:185–189
Manga M, Michaut C (2017) Formation of lenticulae on Europa by saucer-shaped sills. Icarus 286:261–269
Manga M, Wang CY (2007) Pressurized oceans and the eruption of liquid water on Europa and Enceladus. Geophys Res Lett 34(7)
Margot JL, Padovan S, Campbell D, et al (2013) Measurements of the spin states of Europa and Ganymede. In: American Astronomical Society, DPS Meeting
Masters A, Modolo R, Roussos E, et al (2025) Magnetosphere and plasma science with the Jupiter ICy moons Explorer. Space Sci Rev 221(2):24
Mazarico E, Buccino D, Castillo-Rogez J, et al (2023) The Europa Clipper gravity and radio science investigation. Space Sci Rev 219(4):30
McKinnon WB (1997) Mystery of Callisto: is it undifferentiated? Icarus 130(2):540–543
McKinnon WB (2006) On convection in ice I shells of outer Solar System bodies, with detailed application to Callisto. Icarus 183(2):435–450
Meinesz FAV (1950) A remarkable feature of the Earth's topography. NV Noord-Hollandsche Uitgevers Mij
Miyazaki Y, Stevenson DJ (2022) A subsurface magma ocean on Io: exploring the steady state of partially Molten planetary bodies. Planet Sci J 3(11):256
Moore JC (2000) Models of radar absorption in Europan ice. Icarus 147(1):292–300
Moore WB, Schubert G (2000) The tidal response of Europa. Icarus 147(1):317–319
Moore WB, Schubert G (2003) The tidal response of Ganymede and Callisto with and without liquid water oceans. Icarus 166(1):223–226
Mousis O, Schneeberger A, Lunine JI, et al (2023) Early stages of Galilean moon formation in a water-depleted environment. Astrophys J Lett 944(2):L37
Murray CD, Dermott SF (1999). Solar System dynamics. Cambridge University Press
Nadezhdina I, Zubarev A, Kozlova N, et al (2024) JunoPerijove 34: update Ganymede 3D-control network and new DEMs study. Planet Space Sci 252:105981
Nagel K, Breuer D, Spohn T (2004) A model for the interior structure, evolution, and differentiation of Callisto. Icarus 169(2):402–412
Nimmo F (2004a) Non-Newtonian topographic relaxation on Europa. Icarus 168(1):205–208
Nimmo F (2004b) Stresses generated in cooling viscoelastic ice shells: Application to Europa. J Geophys Res Planets 109(E12)
Nimmo F, Thomas PC, Pappalardo RT, et al (2007) The global shape of Europa: constraints on lateral shell thickness variations. Icarus 191(1):183–192
Nimmo F, Bills B, Thomas P (2011) Geophysical implications of the long-wavelength topography of the Saturnian satellites. J Geophys Res Planets 116(E11)
Nimmo F, Canup R, Fujii Y, et al (2026) Origin and evolution of the Galilean satellites within the Jovian system. Space Sci Rev 222
Noir J, Hemmerlin F, Wicht J, et al (2009) An experimental and numerical study of librationally driven flow in planetary cores and subsurface oceans. Phys Earth Planet Inter 173(1):141–152
Oberst J, Schuster P (2004) Vertical control point network and global shape of Io. J Geophys Res Planets 109(E4)
Ogliore R, Burchell MJ, Davis A, et al (2024) Io sample return: a record of planet formation in the outer Solar System. AGU24
Ojakangas GW, Stevenson DJ (1989) Polar wander of an ice shell on Europa. Icarus 81(2):242–270
O'Reilly TC, Davies GF (1981) Magma transport of heat on Io: a mechanism allowing a thick lithosphere. Geophys Res Lett 8(4):313–316
Palguta J, Anderson JD, Schubert G, et al (2006) Mass anomalies on Ganymede. Icarus 180(2):428–441

Panning M, Lekic V, Manga M, et al (2006) Long-period seismology on Europa: 2. Predicted seismic response. J Geophys Res Planets 111(E12)
Pappalardo RT, Collins GC, Head J, et al (2004) Geology of Ganymede. In: Bagenal F, Dowling TE, McKinnon WB (eds) Jupiter: the planet, satellites and magnetosphere. Cambridge University Press, pp 363–396
Pappalardo R, McKinnon W, Khurana K (2009) Europa. Cambridge University Press, Cambridge
Park R, Jacobson R, Gomez Casajus L, et al (2025a) Io's tidal response precludes a shallow magma ocean. Nature 638(8049):69–73
Park R, Berne A, Konopliv A, et al (2025b) Thermal asymmetry in the Moon's mantle inferred from monthly tidal response. Nature 641(8065):1188–1192
Pauer M, Musiol S, Breuer D (2010) Gravity signals on Europa from silicate shell density variations. J Geophys Res Planets 115(E12)
Petrenko V, Whitworth R (1999) Physics of ice. Oxford University Press
Petricca F, Castillo-Rogez JC, Genova A, et al (2025a) Partial differentiation of Europa and implications for the origin of materials in the Jupiter system. Nat Astron 9:501–511
Petricca F, Vance SD, Parisi M, et al (2025b) Titan's strong tidal dissipation precludes a subsurface ocean. Nature 648(8094):556–561
Petricca F, Cochrane C, Cascioli G, et al (2026) Characterization of Europa's interior through synthesis of Europa Clipper data. Planet Sci J
Phua YY, Stevenson DJ (2026) Impact-induced contamination of Ganymede's deep ice shell. Planet Sci J 7(1):7
Prockter LM, Hibbard KE, Magner TJ, et al (2011) Exploring Europa: science from the Jupiter Europa orbiter-a future outer planet flagship mission. Johns Hopkins APL Tech Dig 30(1):72–84
Qin C, Zhong S, Wahr J (2016) Elastic tidal response of a laterally heterogeneous planet: a complete perturbation formulation. Geophys J Int 207(1):89–110
Rambaux N, Van Hoolst T, Karatekin Ö (2011) Librational response of Europa, Ganymede, and Callisto with an ocean for a non-Keplerian orbit. Astron Astrophys 527:A118
Rekier J, Trinh A, Triana SA, et al (2019) Internal energy dissipation in Enceladus's subsurface ocean from tides and libration and the role of inertial waves. J Geophys Res Planets 124(8):2198–2212
Reynard B, Sotin C (2023) Carbon-rich icy moons and dwarf planets. Earth Planet Sci Lett 612:118172
Roberts JH, McKinnon WB, Elder CM, et al (2023) Exploring the interior of Europa with the Europa Clipper. Space Sci Rev 219(6):46
Ross M, Schubert G, Spohn T, et al (1990) Internal structure of Io and the global distribution of its topography. Icarus 85(2):309–325
Roth L, Saur J, Retherford KD, et al (2014) Transient water vapor at Europa's south pole. Science 343(6167):171–174
Roth L, Retherford KD, Saur J, Strobel DF, et al (2026) Europa's Lyman-α emissions from HST/STIS observations. Astron Astrophys
Rovira-Navarro M, Rieutord M, Gerkema T, et al (2019) Do tidally-generated inertial waves heat the subsurface oceans of Europa and Enceladus? Icarus 321:126–140
Rovira-Navarro M, Gerkema T, Maas LR, et al (2020) Tides in subsurface oceans with meridional varying thickness. Icarus 343:113711
Rovira-Navarro M, Matsuyama I, Hay HCC (2023) Thin-shell tidal dynamics of ocean worlds. Planet Sci J 4(2):23
Rovira-Navarro M, Matsuyama I, Berne A (2024) A spectral method to compute the tides of laterally heterogeneous bodies. Planet Sci J 5(5):129
Rovira-Navarro M, Matsuyama I, Dirkx D, et al (2025) Prospects of using tidal tomography to constrain Ganymede's interior. Geophys Res Lett 52:e2025GL114708
Šachl L, Kvorka J, Čadek O, et al (2025) Magnetic field induced by convective flow in Europa's subsurface ocean. Icarus 429:116375
Schenk PM, Bulmer MH (1998) Origin of mountains on Io by thrust faulting and large-scale mass movements. Science 279(5356):1514–1517
Schenk P, Matsuyama I, Nimmo F (2020) A very young age for true polar wander on Europa from related fracturing. Geophys Res Lett 47(17):e2020GL088364
Schenk P, McKinnon W, Moore J, et al (2024) Geology, global characteristics, and future exploration. Ganymede 28:126
Schubert G, Anderson J, Spohn T, et al (2004) Interior composition, structure and dynamics of the Galilean satellites. In: Bagenal F, Dowling TE, McKinnon WB (eds) Jupiter: the planet, satellites and magnetosphere. Cambridge University Press, pp 281–306
Schubert G, Sohl F, Hussmann H (2009) Interior of Europa. In: Pappalardo RT, McKinnon WB, Khurana KK (eds) Europa, pp 353–368

Seufert M, Saur J, Neubauer FM (2011) Multi-frequency electromagnetic sounding of the Galilean moons. Icarus 214(2):477–494
Showman AP, Stevenson DJ, Malhotra R (1997) Coupled orbital and thermal evolution of Ganymede. Icarus 129(2):367–383
Soderlund KM (2019) Ocean dynamics of outer Solar System satellites. Geophys Res Lett 46(15):8700–8710
Soderlund KM, Schmidt BE, Wicht J, et al (2014) Ocean-driven heating of Europa's icy shell at low latitudes. Nat Geosci 7:16–19
Soderlund KM, Kalousová K, Buffo JJ, et al (2020) Ice-ocean exchange processes in the Jovian and Saturnian satellites. Space Sci Rev 216(5):1–57
Soderlund KM, Rovira-Navarro M, Le Bars M, et al (2024) The physical oceanography of ice-covered moons. Annu Rev Mar Sci 16(1):25–53
Soderlund KM, Stanley S, Cao H, et al (2025) Puzzles in planetary dynamos: implications for planetary interiors. Annu Rev Earth Planet Sci 53:305–337
Solomatov V (1995) Scaling of temperature-and stress-dependent viscosity convection. Phys Fluids 7(2):266–274
Steinbrügge G, Stark A, Hussmann H, et al (2015) Measuring tidal deformations by laser altimetry. A performance model for the Ganymede Laser Altimeter. Planet Space Sci 117:184–191
Steinbrügge G, Schroeder DM, Haynes MS, et al (2018) Assessing the potential for measuring Europa's tidal Love number h2 using radar sounder and topographic imager data. Earth Planet Sci Lett 482:334–341
Steinbrügge G, Park RS, Roberts JH, Bland M, Brooks S, et al (2026) Geodetic investigations of the Europa Clipper Mission. Space Sci Rev 222:17
Sun S, Yan J, Gao W, et al (2026) Gravity field estimation of Callisto using tracking data for the upcoming Tianwen-4 mission. Acta Astronaut 241:181–191
Takei Y (2017) Effects of partial melting on seismic velocity and attenuation: a new insight from experiments. Annu Rev Earth Planet Sci 45(1):447–470
Thomas P, Davies M, Colvin T, et al (1998) The shape of Io from Galileo limb measurements. Icarus 135(1):175–180
Thomas PC, Tajeddine R, Tiscareno MS, et al (2016) Enceladus's measured physical libration requires a global subsurface ocean. Icarus 264:37–47
Tricarico P (2014) Multi-layer hydrostatic equilibrium of planets and synchronous moons: theory and application to Ceres and to Solar System moons. Astrophys J 782(2):99
Trinh KT, Bierson CJ, O'Rourke JG (2023) Slow evolution of Europa's interior: metamorphic ocean origin, delayed metallic core formation, and limited seafloor volcanism. Sci Adv 9(24):eadf3955
Trumbo SK, Brown ME, Hand KP (2019) Sodium chloride on the surface of Europa. Sci Adv 5(6):eaaw7123
Turcotte D, Willemann R, Haxby W, et al (1981) Role of membrane stresses in the support of planetary topography. J Geophys Res, Solid Earth 86(B5):3951–3959
Turtle EP, Pierazzo E (2001) Thickness of a Europan ice shell from impact crater simulations. Science 294(5545):1326–1328
Tyler RH (2008) Strong ocean tidal flow and heating on moons of the outer planets. Nature 456(7223):770–772
Tyler R (2011a) Tidal dynamical considerations constrain the state of an ocean on Enceladus. Icarus 211(1):770–779
Tyler RH (2011b) Magnetic remote sensing of Europa's ocean tides. Icarus 211(1):906–908
Tyler RH, Maus S, Lühr H (2003) Satellite observations of magnetic fields due to ocean tidal flow. Science 299(5604):239–241
Van Hoolst T, Rambaux N, Karatekin Ö, et al (2008) The librations, shape, and icy shell of Europa. Icarus 195(1):386–399
Van Hoolst T, Baland RM, Trinh A (2013) On the librations and tides of large icy satellites. Icarus 226(1):299–315
Van Hoolst T, Baland RM, Trinh A, et al (2020) The librations, tides, and interior structure of Io. J Geophys Res Planets 125(8):e2020JE006473
Van Hoolst T, Tobie G, Vallat C, et al (2024) Geophysical characterization of the interiors of Ganymede, Callisto and Europa by ESA's Jupiter ICy moons Explorer. Space Sci Rev 220(5):54
Vance S, Harnmeijer J, Kimura J, et al (2007) Hydrothermal systems in small ocean planets. Astrobiology 7(6):987–1005
Vance S, Bouffard M, Choukroun M, et al (2014) Ganymede's internal structure including thermodynamics of magnesium sulfate oceans in contact with ice. Planet Space Sci 96:62–70
Veeder GJ, Matson DL, Johnson TV, et al (1994) Io's heat flow from infrared radiometry: 1983–1993. J Geophys Res Planets 99(E8):17095–17162
Volwerk M, McGrath M, Jia X, et al (2025) Ganymede. Cambridge University Press, Cambridge

Wahr J, Zuber M, Smith DE, et al (2006) Tides on Europa, and the thickness of Europa's icy shell. J Geophys Res Planets 111(E12)
Wahr J, Pappalardo RT, Barr AC, et al (2009) Modeling stresses on satellites due to nonsynchronous rotation and orbital eccentricity using gravitational potential theory. Icarus 200(1):188–206
Wakita S, Johnson BC, Silber EA, et al (2024) Multiring basin formation constrains Europa's ice shell thickness. Sci Adv 10(12):eadj8455
Williams JG, Boggs DH, Yoder CF, et al (2001) Lunar rotational dissipation in solid body and Molten core. J Geophys Res Planets 106(E11):27933–27968
Williams JG, Konopliv AS, Boggs DH, et al (2014) Lunar interior properties from the grail mission. J Geophys Res Planets 119(7):1546–1578
Wilson A, Kerswell RR (2018) Can libration maintain Enceladus's ocean? Earth Planet Sci Lett 500:41–46
Wisdom J (2008) Tidal dissipation at arbitrary eccentricity and obliquity. Icarus 193(2):637–640
Wunsch C, Ferrari R (2004) Vertical mixing, energy and thegeneral circulation of the oceans. Annu Rev Fluid Mech 36:281–314
Yseboodt M, Baland RM (2026) Transformation of orientation and rotation angles of synchronous satellites: application to the Galilean moons. Icarus 450:116977
Zambon F, Mura A, Lopes R, et al (2023) Io hot spot distribution detected by Juno/JIRAM. Geophys Res Lett 50(1):e2022GL100597
Zeng Y, Jansen MF (2024) The effect of salinity on ocean circulation and ice–ocean interaction on Enceladus. Planet Sci J 5(1):13
Zhang Y, Kang W, Marshall J (2024) Ocean weather systems on icy moons, with application to Enceladus. Sci Adv 12(15):38
Zharkov V (2004) A theory of the equilibrium figure and gravitational field of the Galilean satellite Io: the second approximation. Astron Lett 30(7):496–507
Zharkov V, Gudkova T (2010) Models, figures and gravitational moments of Jupiter's satellite Io: effects of the second order approximation. Planet Space Sci 58(10):1381–1390
Zharkov V, Karamurzov B (2006) Models, figures, and gravitational moments of Jupiter's satellites Io and Europa. Astron Lett 32:495–505
Zharkov V, Leontjev V, Kozenko A (1985) Models, figures, and gravitational moments of the Galilean satellites of Jupiter and icy satellites of Saturn. Icarus 61(1):92–100
Zhu P, Manucharyan GE, Thompson AF, et al (2017) The influence of meridional ice transport on Europa's ocean stratification and heat content. Geophys Res Lett 44(12):5969–5977
Zimmer C, Khurana KK, Kivelson MG (2000) Subsurface oceans on Europa and Callisto: constraints from Galileo magnetometer observations. Icarus 147(2):329–347
Zubarev A, Nadezhdina I, Oberst J, et al (2015) New Ganymede control point network and global shape model. Planet Space Sci 117:246–249

Publisher's Note Springer Nature remains neutral with regard to jurisdictional claims in published maps and institutional affiliations.

Authors and Affiliations

Francis Nimmo[1] · Anton Ermakov[2] · Wanying Kang[3] · Marc Rovira-Navarro[4] · Gabriel Tobie[5] · Tim Van Hoolst[6,7]

✉ M. Rovira-Navarro
M.RoviraNavarrao@tudelft.nl

F. Nimmo
fnimmo@ucsc.edu

A. Ermakov
aie@stanford.edu

W. Kang
wanying@mit.edu

G. Tobie
gabriel.tobie@univ-nantes.fr

T. Van Hoolst
tim.vanhoolst@oma.be

1 Department of Earth and Planetary Sciences, University of California Santa Cruz, 1156 High St, Santa Cruz, CA 95064, USA

2 Department of Aeronautics and Astronautics, Stanford University, 496 Lomita Mall, Stanford, 94305, USA

3 Department of Earth, Atmopshere and Planetary Sciences, MIT, 21 Ames street, Cambridge, 02139, USA

4 Delft University of Technology, Kluyverweg 1, Delft, 2629HS, the Netherlands

5 Laboratoire de Planétologie et Géosciences, LPG UMR 6112, Nantes Université, Univ Angers, Le Mans Université, CNRS, 2 rue de la Houssiniere, Nantes, 44000, France

6 Royal Observatory of Belgium, Ringlaan 3, Brussels, 1180, Belgium

7 Institute of Astronomy, KU Leuven, Celestijnenlaan 200D, Leuven, 3001, Belgium